

This dissertation has been
microfilmed exactly as received

70-4463

CORVIN, Kalman Kutszegi, 1932-
MOLECULAR DISSOCIATION OF CARBON
DIOXIDE AND WATER VAPOR BY
ELECTRON SWARMS OF A UNIFORM
POSITIVE COLUMN.

The University of Oklahoma, Ph.D., 1969
Physics, nuclear
University Microfilms, Inc., Ann Arbor, Michigan

THE UNIVERSITY OF OKLAHOMA

GRADUATE COLLEGE

MOLECULAR DISSOCIATION OF CARBON DIOXIDE AND WATER VAPOR

BY ELECTRON SWARMS OF A UNIFORM POSITIVE COLUMN

A DISSERTATION

SUBMITTED TO THE GRADUATE FACULTY

in partial fulfillment of the requirements for the

degree of

DOCTOR OF PHILOSOPHY

by

KALMAN KUTSZEGI CORVIN

Norman, Oklahoma

1969

MOLECULAR DISSOCIATION OF CARBON DIOXIDE AND WATER VAPOR
BY ELECTRON SWARMS OF A UNIFORM POSITIVE COLUMN

A DISSERTATION

APPROVED FOR THE DEPARTMENT OF PHYSICS

APPROVED BY:

Robert M. St. John
Richard Broecker
Balfour S. Whitney
John J. Carroll
Paul A. Day

DISSERTATION COMMITTEE

ACKNOWLEDGEMENTS

It is indeed a pleasure to express thanks and sincere appreciation to Professor Robert M. St. John for his patient and helpful supervision of the effort presented here.

Special thanks are due to Dr. S.J.B. Corrigan: this work began under his guidance during his stay as a visiting professor. Even after his return to England he managed to slip some useful advice across the ocean.

The author is grateful to all his friends and colleagues for all the casual conversations that have averted many small crises in the course of the experiments, and that, one way or another, assisted and encouraged the progress of these efforts. The enlightening and helpful discussions with Dr. R. H. Lynch are especially noted.

TABLE OF CONTENTS

	Page
ACKNOWLEDGEMENT	iii
LIST OF TABLES.	vi
LIST OF ILLUSTRATIONS	vii
 Chapter	
I. INTRODUCTION	1
The Theoretical Basis for the Dissociation Experiments	6
II. EXPERIMENTAL METHOD.	10
The Dissociation Coefficient in Terms of Experi- mental Parameters	11
The Apparatus	14
Method of Observation	18
III. REMARKS ON THE UNIFORM POSITIVE COLUMN IN CARBON DI- OXIDE AND WATER VAPOR.	26
IV. PRESENTATION AND DISCUSSION OF RESULTS	34
The Rate Coefficient of Dissociation for CO ₂	35
Dissociation Mechanism for CO ₂	45
The Rate Coefficients for H ₂ O Vapor	49
Dissociation Processes in H ₂ O	62

TABLE OF CONTENTS (Continued)

Chapter	Page
V. DISSOCIATION CROSS SECTION CALCULATED FROM SWARM DATA	68
The Relation Between the Rate Coefficient and the Cross Section	
The Dissociation Cross Section of CO ₂	73
VI. SUMMARY.	77
LIST OF REFERENCES.	80

LIST OF TABLES

Table	Page
1. Dissociation coefficients for carbon dioxide from the observations on the rates of increase of noncondensable dissociation products in a segment Δl of the positive column.	39
2. Dissociation coefficients for carbon dioxide obtained by measuring the changes in $\Delta(\text{CO}_2)/\Delta t$ with respect to l , and subsequently recalculated by considering the rates of appearance of permanent gas products only and using Eq. (IV.4).	43
3. Dissociation coefficients for water vapor obtained from the observed rates of increase of permanent gas products in a segment Δl of the positive column.	57
4. Dissociation coefficients for water vapor from the slopes of the $\Delta(\text{H}_2\text{O})/\Delta t$ vs. l plots.	59
5. Dissociation coefficients of water vapor on the basis of the reaction mechanism suggested by Figs. 12 and 13 and the corresponding expression for $\alpha = f(E/p)$ given in Eq. (IV.2).	60
6. Dissociation coefficients of water vapor with a variation in the discharge current, measured by the same method as those listed in Table 5	61

LIST OF ILLUSTRATIONS

Figure	Page
1. The Schematic Diagram of the Discharge Tube and the Associated Electrical Circuits	15
2. The Regulator Circuit.	19
3. The Dependence of E/p on pR for CO_2 Measured at a Discharge Current of 0.6 mA and a Tube Radius of 1.25 cm	32
4. The Dependence of E/p on pR for H_2O Vapor at Discharge Currents Between 0.3 and 0.7 mA and a Tube Radius of 1.25 cm	33
5. The Pressure Changes ΔP and Δp Plotted as a Function of Time for $p_0 = 1.23$ Torr of CO_2 , at $i = 0.6$ mA and an E/p of $18.6 \text{ v}\cdot\text{cm}^{-1}\cdot\text{Torr}^{-1}$	36
6. The Pressure Changes ΔP and Δp Plotted as a Function of Time for $p_0 = 3.08$ Torr of CO_2 and $i = 0.6$ mA, $E/p = 11.2 \text{ v}\cdot\text{cm}^{-1} \text{ Torr}^{-1}$	37
7. The Rate of Disappearance of CO_2 Molecules Due to Dissociation as a Function of Positive Column Length for $p_0 = 2.06$ Torr and $i = 0.6$ mA.	41
8. The Rate Coefficient of Dissociation for CO_2 as a Function of E/p_0	44
9. The Rate Coefficient for Dissociative Attachment in CO_2 , α_a/p Calculated from the Cross Sections Measured by Rapp and Briglia.	48
10. An Example Showing the Rate of Adsorption of Water Vapor in the Discharge Vessel at 25° C	50
11. The Adsorption Rate - $\delta P/\delta t$ Plotted Against the Pressure Averaged Over the Corresponding Time Interval.	52
12. The Time Rate of Change of ΔP and Δp for 0.54 Torr of Water Vapor at a Current of 0.5 mA and an E/p of $42 \text{ v}\cdot\text{cm}^{-1}\cdot\text{Torr}^{-1}$	54

LIST OF ILLUSTRATIONS (Continued)

Figure	Page
13. The Time Rate of Change of ΔP and Δp for 3.08 Torr of H_2O Vapor at an E/p of $35.7 \text{ v}\cdot\text{cm}^{-1}\cdot\text{Torr}^{-1}$	55
14. The Dissociation Coefficient of H_2O Vapor as a Function of E/p	63
15. A Comparison of Dissociation Coefficients with Coefficients of Dissociative Attachment and Ionization.	66
16. The Estimated Electron-Impact Dissociation Cross Section for CO_2 as a Function of Electron Energy E	76

MOLECULAR DISSOCIATION OF CARBON DIOXIDE AND WATER VAPOR
BY ELECTRON SWARMS OF A UNIFORM POSITIVE COLUMN

CHAPTER I

INTRODUCTION

Electrons moving in molecular gases may often encounter molecules such that the resulting effect is some type of a change in the chemical constitution of the gas. It is clear, however, that a distinction between "chemical" or "physical" changes caused by such electronic collisions serves no useful purpose. It was recognized early⁽¹⁾ that a chemical reaction brought about by electron impact is intimately related to the mechanism which establishes the electron-molecule interaction. Namely, ionization by electron impact in low current-density swarms was construed as a reaction that could be expressed in quantitative terms as a rate coefficient, known now as Townsend's α , giving the number of ion pairs generated by an electron per unit displacement in the direction of applied field.

This approach eventually gained a wider ground in the interpretation of the ionization coefficient advanced by Emeléus, Lunt, and Meek⁽²⁾. Their theory, constructed from considerations based on simple kinetic theory, is remarkable in that it successfully inter-related such average quantities characteristic of electrical discharges

as the rate coefficients and information on single collision events assuming that the electron energy distribution could be inferred in some way. The theory was further developed^(3,4) to encompass electronic excitation processes including those leading to dissociation. The experiments presented in this dissertation lean heavily on the conceptual foundations offered by this theory.

Attention in the present work is focused on one particular kind of inelastic collision between electrons and molecules: molecular dissociation into electrically neutral fragments. This type of excitation by electron impact may proceed by one or both of the following processes:

(i) by a direct excitation to an unstable electronic state in which the molecule spontaneously dissociates, and

(ii) by an excitation to a bound state with a subsequent transition to an unstable state which results in dissociation.

Observation of the excitation of the first kind is necessarily difficult since such a route is not accompanied by an emission of radiation, thus, it cannot be detected by photometric means. This difficulty is the reason why dissociation into uncharged fragments is the least explored of all excitation processes.

Only the dissociative excitation of the hydrogen molecule has been investigated in a considerable number of single-event observations. Poole⁽⁵⁾ measured the production rate of hydrogen atoms in the positive column of a glow discharge using a stream of molecular

gas. By means of calorimetric methods he obtained the energy efficiency (more appropriately called the energy yield for dissociation) in terms of the number of dissociated molecules arriving as atoms at the calorimeter per unit of energy supplied to the positive column.

These measurements and further experiments in r-f discharges^(6,7) have demonstrated that as much as half of the electrical energy supplied to the discharge is expended in dissociative excitation. A major significance of these findings is that the production of the atoms cannot be explained if ionization is assumed to be involved as the main atom-producing mechanism.

An energy-dependent cross section for the dissociation of molecular hydrogen was measured by Corrigan⁽⁸⁾ whose experiment yielded the only directly measured cross section of the kind to date. His experiment employed a chemical trapping technique making use of molybdenum trioxide, a substance known to absorb atomic hydrogen with an efficiency of unity per collision while it does not react with the molecules at room temperature. The dissociative excitation of molecules was achieved by electrons of controlled energy under conditions such that only binary collisions with the gas molecules were important.

The numerical values obtained for the energy yield of the dissociative transition of molecular hydrogen from the ground state to the non-radiating repulsive state on one hand, and the directly measured cross section as a function of energy on the other, have shown the general nature of the process involved. The neutral hydrogen

molecule being in its ground state $1\Sigma_g^+$ may be excited to the repulsive triplet state $1^3\Sigma_u^+$ immediately above it, going to the same dissociation limit (at 4.48 eV) as the ground state. At higher energies there is a sequence of states which lie in the Franck-Condon interaction region. Since triplet-to-singlet intercombination lines do not exist in the spectrum of molecular hydrogen, it follows that excitation by electron impact to any triplet state must result in dissociation. Thus, dissociation may proceed either directly by the transition $1\Sigma_g^+ \rightarrow 1^3\Sigma_u^+$ or by way of radiative cascading from the higher triplet levels to the repulsive $1^3\Sigma_u^+$ state. This picture gives a hint of the complexity of problems surrounding the attempts to observe neutral-fragment dissociation.

In addition to the past work cited above, mention must be made of a crossed-beam technique devised by Corrigan⁽⁹⁾. The method, currently being developed, is based on the fact that since dissociative excitation takes place in accordance with the Franck-Condon principle, the energy imparted to the molecule is greater than the molecular dissociation energy. Then, the molecular fragments carry off the excess energy of the excited molecule in kinetic form. When a molecular beam of thermal energy and a stream of electrons are crossed, a suitable measurement of the dissociation products scattered at random can lead to a quantitative determination of the dissociation rate in the beam. This method does not hinge upon a detailed knowledge of the chemical processes in which the dissociation products are involved.

Much work has been done on the chemistry of electrical discharges⁽¹⁰⁾, but quantitative information on absolute rates of chemical reactions induced by electron collisions is rather scarce. The mechanism of impact reactions, clearly in many cases, can be explained in terms of dissociation into neutral fragments. If the cross sections for these reactions are large enough for the range of electronic energies available in the discharge, the overall reaction mechanisms cannot be understood without the knowledge of these cross sections.

It will be demonstrated later that the physical and technical operation of electrical discharges, specifically the behavior of the uniform positive column of d-c glow discharges in molecular gases is strongly determined by the process of dissociation. Furthermore, the full appraisal of the operational qualities of molecular gas lasers and a physical understanding of inversion mechanisms occurring in these devices demand the knowledge of dissociation cross sections⁽¹¹⁾. Also, these cross sections play an important role in the understanding of the interaction of high-energy radiation with matter. The secondary electrons of comparatively low energy arising from such an interaction may initiate the production of free atoms and radicals. Data provided by low-energy collision experiments may then be instrumental in shedding light on those problems in high-energy radiation chemistry or astrophysics which implicate dissociative excitation. Thus, studies of low-energy dissociating collisions may have a wide range of applications beyond the conventional discipline of discharge chemistry.

The Theoretical Basis for the Dissociation Experiments

Before proceeding to a description of the present work on the dissociation of carbon dioxide and water vapor, the concepts which predetermined the particular experimental design will be discussed. As it was noted, a direct measurement of the cross section for a given electron-impact process requires (a) a definite current of electrons given in a mono-energetic beam, and (b) a method to ascertain the number of collision events of a given process in a given time. Beside the great difficulties already cited with respect to the requirement in (b), there are also considerable difficulties in establishing an electron current of sufficiently controlled energy since the cross section for an electronic excitation of the type investigated often spans a range of the order of, or less than ten electron-volts.

A direct measurement of the cross section for dissociation, or for any other process, by electron impact is not possible in electrical discharges in which a swarm of electrons moves in equilibrium with a uniform field because the electrons have a wide spread of energies.

Electrons drifting in a gas under the influence of an electric field undergo many collisions with the gas molecules and acquire, as a result of these encounters, large random components of velocity in addition to their drift speed in the field direction. The experiments of Townsend and his collaborators⁽¹²⁾ have demonstrated that the random

velocities of electrons in the swarm are much greater than those corresponding to the temperature of the gas molecules. Since in a steady-state swarm the energy gain of an electron per mean free path must be equal to the average fractional energy loss per collision, the mean value of random velocities, \bar{v} , can be shown to be dependent upon the ratio of electric field E to the gas pressure p . Hence, $\bar{v} = f(E/p)$ provided that the average drift velocity of electrons, w , is also a function of E/p . This has been shown to be the case in experiments on the drift of electrons in electric fields⁽¹³⁾. Hence, it can be concluded that rate processes governed by mean electron energy in a given gas are dependent on the parameter E/p .

A complete analysis of swarm processes which shows the relationship between the average properties of a swarm and the scattering of individual electrons in single encounters seems to be possible in principle⁽¹⁴⁾, but the empirical and mathematical difficulties arising from such an esoteric approach are all too often overwhelming. The simple theory of Emeléus, Lunt and Meek⁽²⁻⁴⁾, evading such depths of the problem and still succeeding in showing the connection between average swarm properties and single collision events, has shown that collision processes produced by a swarm can be determined by means of a rate coefficient. The data necessary to describe these processes consist of those giving the electronic energy distribution in the swarm for which the average properties have been measured. The rate coefficient, the number of events as a result of a given collision process

per unit volume per unit time, is given as

$$R = k p n_e \int_0^{\infty} Q(\epsilon) \epsilon^{1/2} f(\epsilon) d\epsilon ,$$

where n_e is the electron concentration, p is the gas pressure (which is a measure of molecule concentration), $Q(\epsilon)$ is the cross section for the process, $f(\epsilon)$ the electronic energy distribution, and k is a numerical factor depending on the units used. If the shape of the distribution function $f(\epsilon)$ can be plausibly assumed, then the values of electron temperatures and drift velocities, all expected to be known from experiment over the desired ranges of E/p , enable one to find the interrelation between the rate coefficients and the corresponding cross section.

Therefore, electronic collision processes brought about by a swarm can be measured in terms of a rate coefficient defined as the number of events produced by an electron in drifting unit distance in the direction of applied electric field. In turn, the dependence of the rate coefficient on average quantities, such as the discharge current and the applied field, can be determined. Then, if the electronic energy distribution present in the low-current density swarm can be inferred, the absolute magnitude of the cross section for a particular excitation process as a function of electron energy can be estimated from the rate-coefficient data.

In the present work the rate coefficient of dissociation characterizing the electron swarm of a d-c positive column was

determined in carbon dioxide and water vapor by separating the condensable parent molecules from the permanent products formed in the discharge. As shown by the results of these experiments, a first-order reaction could be concluded for the collision reactions in CO_2 and H_2O . The overlap integral expressing the connection between the dissociation coefficient and the cross section for dissociative excitation (formally similar to the integral shown above) is derived in Chapter V in a form best-suited for the results of the experiments presented here. The specific conditions that enabled the attainment of dissociation coefficients in a positive-column experiment will be enumerated in the following chapter.

CHAPTER II

EXPERIMENTAL METHOD

In the highly intricate structure of a d-c glow discharge the homogeneous (i.e., the nonstriated and nonconstricted) positive column is prominently characterized by the fact that its condition is the same at various distances from the cathode. If the potential across the discharge tube is measured while the length of the positive column is varied by means of a movable anode, and if the other discharge parameters remain constant, then one obtains a constant increment of potential difference per unit increment of positive column length. Since the electrons drifting through the column receive their energy from a constant electric field, the electronic energy distribution in the positive column is independent of position along the axis of the discharge tube. Consequently, if the positive column is uniform, that is, if the swarm of electrons in the column moves under the influence of a uniform electric field, then a quantitative investigation of the rate of an electron-impact reaction can be made in the positive column of a glow discharge.

In addition, sufficiently low values of current density in the positive column must be stipulated. If the current density is low, then the stationary concentration of ions and excited species, all products of electron collisions, will be negligible in comparison with the ground-state concentration of gas molecules. Hence, secondary effects will be negligible.

The design of the experiment outlined here was largely determined by these two requirements. Both conditions, the requirement of a steady-state positive column and that of a low-current-density swarm, were imposed to assure intelligible observations, and to assure that the average properties of the given rate process could be related to single collision events between electrons and molecules.

The Dissociation Coefficient in Terms of Experimental Parameters

In order to determine the magnitude of the rate coefficient for molecular dissociation, the coefficient must be expressed in terms of quantities that can be measured in a positive-column experiment. Furthermore, to evaluate a dissociation coefficient, the number of molecules dissociated in a given time interval must be determined.

It will be shown later that the dissociation of both carbon dioxide and water vapor leads to permanent gaseous products. One cannot, therefore, immediately identify total pressure changes with changes in the number of molecules present. The total pressure change will be determined by the difference between the gaseous product molecules formed by the dissociation fragments and the number of molecules

lost by dissociation. In the case of the present work it is possible to separate these contributions to the total pressure change by condensing the remaining molecular gas in a liquid-nitrogen trap. Accordingly, the number of molecules n dissociated can be identified as a change in the gas pressure p , i.e.,

$$\Delta n \propto \Delta p(M) . \quad (\text{II.1})$$

(Here M denotes the molecular gas of interest and becomes specified only when the results on the gases investigated, CO_2 and H_2O , are presented.)

Providing that the current density in the positive column is sufficiently low, so that multistage excitation processes are excluded, the molecular dissociation rate per unit column length must be proportional to the electron current i for constant reduced field E/p . Hence, if $(\Delta n/\Delta t)$ is denoted as $\Delta \dot{n}$,

$$\frac{\Delta \dot{n}}{\Delta l} \propto i . \quad (\text{II.2})$$

If the proportionality constant in Eq. (II.2) is α_d , the rate coefficient (in events/electron·cm drift), the dissociation rate is given by

$$\Delta \dot{n} = \alpha_d \frac{i \Delta l}{e} \quad (\text{sec}^{-1}) \quad (\text{II.3})$$

where the current i is in amperes, and e is the charge of an electron, 1.602×10^{-19} coulomb.

If the number of molecules in a closed vessel of volume B cm³ changes by Δn in a time interval Δt , the rate of change in the number of molecules is expressed in terms of the resulting pressure change Δp_o by

$$\Delta \dot{n} = B \left(\frac{n_o}{p_s} \right) \frac{\Delta p_o}{\Delta t} , \quad (\text{II.4})$$

where n_o is the Loschmidt number (26.87×10^{18} cm⁻³) at 0° C and at $p_s = 760$ Torr. The measured pressure change Δp is reduced to conform with the standard conditions and is written as Δp_o .

Equating the two expressions for $\Delta \dot{n}$ in Eq. (II.3) and Eq. (II.4) yields an equation for the rate coefficient of dissociation:

$$\frac{\alpha_d}{p_o} = 5.66 \times 10^{-3} \frac{B}{i \Delta \ell p_o} \left[\frac{\Delta p_o (M)}{\Delta t} \right] \quad (\text{II.5})$$

(electron⁻¹ · cm⁻¹ · Torr⁻¹),

in which $\Delta p_o (M) / \Delta t$ is the observed rate of disappearance of molecules by electron-impact dissociation, in a length $\Delta \ell$ of positive column carrying a current of i amperes.

It may be noted here that, since the drift velocity of free electrons is much greater than that of the more massive positive ions, the whole tube current may be taken as equal to the positive-column electron current with negligible error.

Thus, Eq. (II.5) gives, in terms of quantities all measurable, the number of events leading to molecular dissociation caused by an electron drifting through unit distance in the potential gradient of the positive column per unit pressure of the gas.

The Apparatus

The dissociation coefficient was measured by means of an apparatus consisting essentially of a cylindrical discharge tube with a movable anode to vary the length of the positive column. A schematic diagram of the experimental arrangement is shown in Fig. 1. The discharge tube attached to a conventional vacuum system, the liquid nitrogen trap T, and the oil manometer M are the major components of the apparatus.

The discharge tube and the adjoining vacuum system were made of pyrex glass. The mercury diffusion pump was separated from the tube by a mercury trap of special design and a liquid-nitrogen trap connected in series. The system could be evacuated to pressures of the order of 10^{-6} Torr through a metal valve S_1 , with reasonable rapidity. The inside walls of the tube were cleaned of the possibly adherent gases by heating tapes or a vigorous discharge of a high-frequency spark coil. The gases under investigation were admitted from reservoirs in any desired dosage through a tight needle valve S_2 . Thus, greased stopcocks were eliminated because of their irrepressible tendency to leak when frequently in use.

The liquid-nitrogen trap attached to the discharge tube served the purpose of freezing out the molecular gas remaining in the tube after the termination of discharge, so that the partial pressure of the permanent (i.e., the noncondensable) dissociation products could be determined. Carbon dioxide, one of the molecular gases investigated,

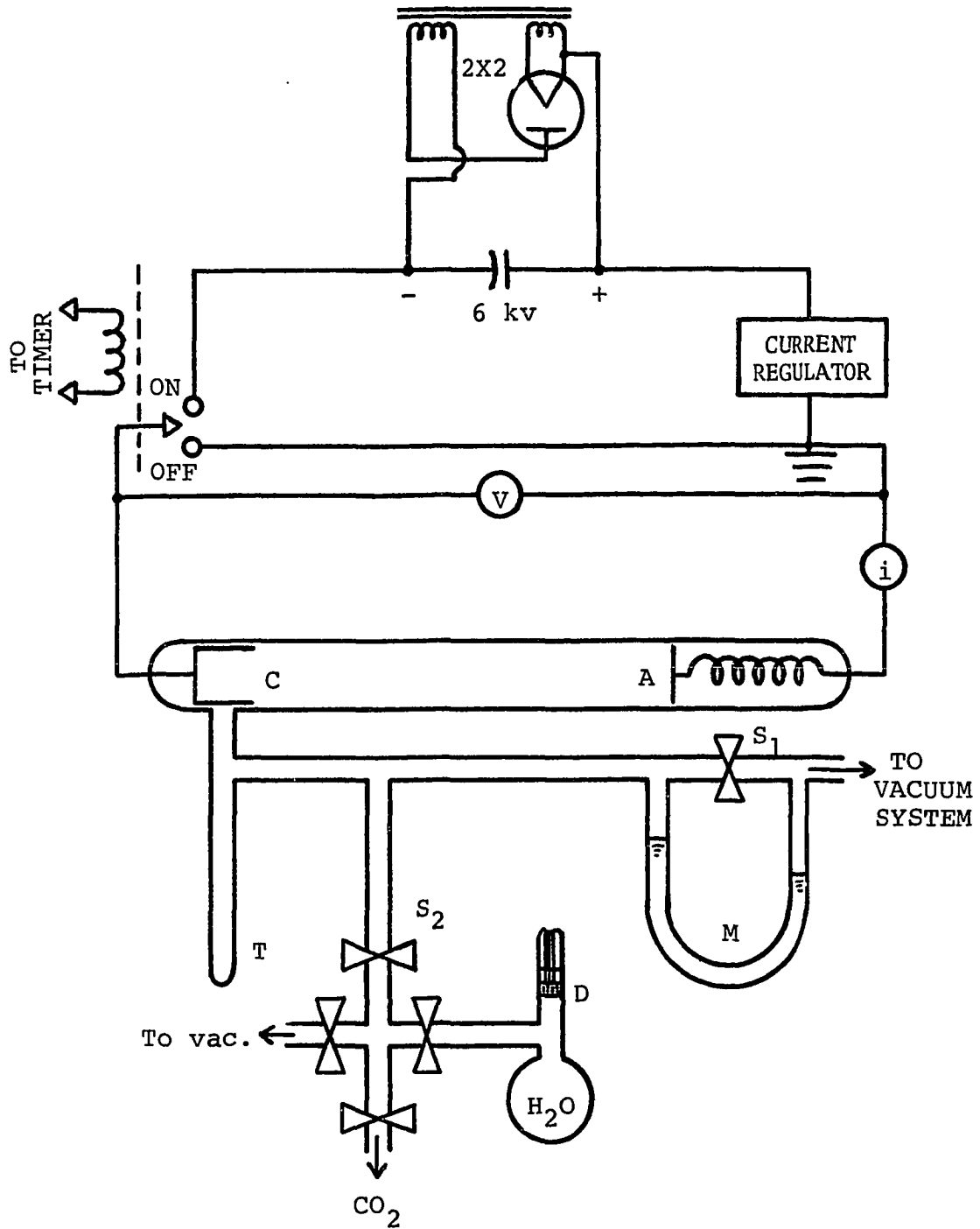


FIGURE 1. The Schematic Diagram of the Discharge Tube and the Associated Electrical Circuits.

was taken from a lecture bottle; the reservoir of distilled water was a previously evacuated bulb into which the water entered through a capillary tube touching a disk D of fine porosity while the disk was covered with a layer of mercury. The samples of the gas admitted into the tube were freed of traces of noncondensable impurities by a freeze-out followed by an evacuation.

The discharge tube was 2.5 cm in diameter and had a hollow cathode and an axially movable anode which almost filled the cross section of the tube. The electrodes were made of tantalum.

It is known that the positive column is not essential to maintain a glow discharge: if the distance between two plane electrodes is reduced to the extent of the dark spaces and the negative glow, the positive column will disappear, and the glow discharge still remains. On a reduction in electrode spacing to the extent of the Crookes dark space, the potential across this space, known as the cathode fall, is found. Even for a fully structured glow discharge, the cathode fall may be a large part of the total interelectrode potential. (The negative glow and the Faraday dark space are more or less field-free regions.)

These complications can be circumvented in part by the application of a hollow cathode which is known to compress the dark regions so that practically all the space between the electrodes is filled with the positive column. Nevertheless, the cathode fall of potential is contracted in space, not much in magnitude. In order to find the

axial electric field in the positive column, it is still necessary to subtract the cathode and anode falls from the total potential drop across the tube. The anode was connected inside the tube through a tungsten coil that permitted it to be moved along the tube at will by an external magnet.

Pressures were measured with an oil manometer, constructed of a 1 cm bore tube and capable of indicating pressures in the range from 1 milliTorr to 10 Torr, which were read with the aid of a cathetometer equipped with a micrometer eyepiece. The stopcock customarily intervening between the two arms of a manometer was eliminated by joining the reference arm directly to the diffusion pump via the mercury traps of the vacuum system. This modification proved to be advantageous not only because another greased stopcock was removed, but also because some of the gas inevitably dissolved in the manometer oil might have sporadically evolved into the space of the closed end.

The most favorable choice of manometer oil was found to be Octoil-S. This is the least viscous of the high-quality pump fluids available to produce the greatest manometer displacement; it allows a 17 per cent improvement over the next best choice of the often-used DC-704.

The electrical circuits schematically shown in the diagram of Fig. 1 were constructed such that the discharge current i could be kept constant at an order of 1 mA, or less, while the potential V was

measured for various lengths of the positive column with a high-impedance d-c voltmeter (100 K Ω per volt). The tube current was supplied by a 6-kV power pack through a series regulator. In this device a vacuum tube was connected to act effectively as a variable resistor in series with the discharge current. The potential difference due to the discharge current across a variable resistor was compared with a reference voltage supplied by a dry battery, and the resulting error signal was amplified and applied as negative feedback to the grid of the regulator tube. Thus, changes in the discharge current caused by quite large variations in the discharge voltage were made insignificantly small. The current was set to the required value by the adjustment of the variable resistor across which the regulator error signal was developed. The regulator circuit is shown in the diagram of Fig. 2.

Method of Observation

It was found that steady positive columns suitable for dissociation measurements could be obtained for initial pressures of CO₂ between about 0.3 and 4 Torr, for H₂O vapor between 0.4 and 3.8 Torr. It was possible to obtain reasonably steady columns for water vapor up to 5 Torr only for short (about 10-15 cm) interelectrode lengths. For this reason, and since for relatively large pressure changes there is but small corresponding change in E/p, the pressure region between 3.8 and 5 Torr in H₂O vapor was ignored in the dissociation measurements.

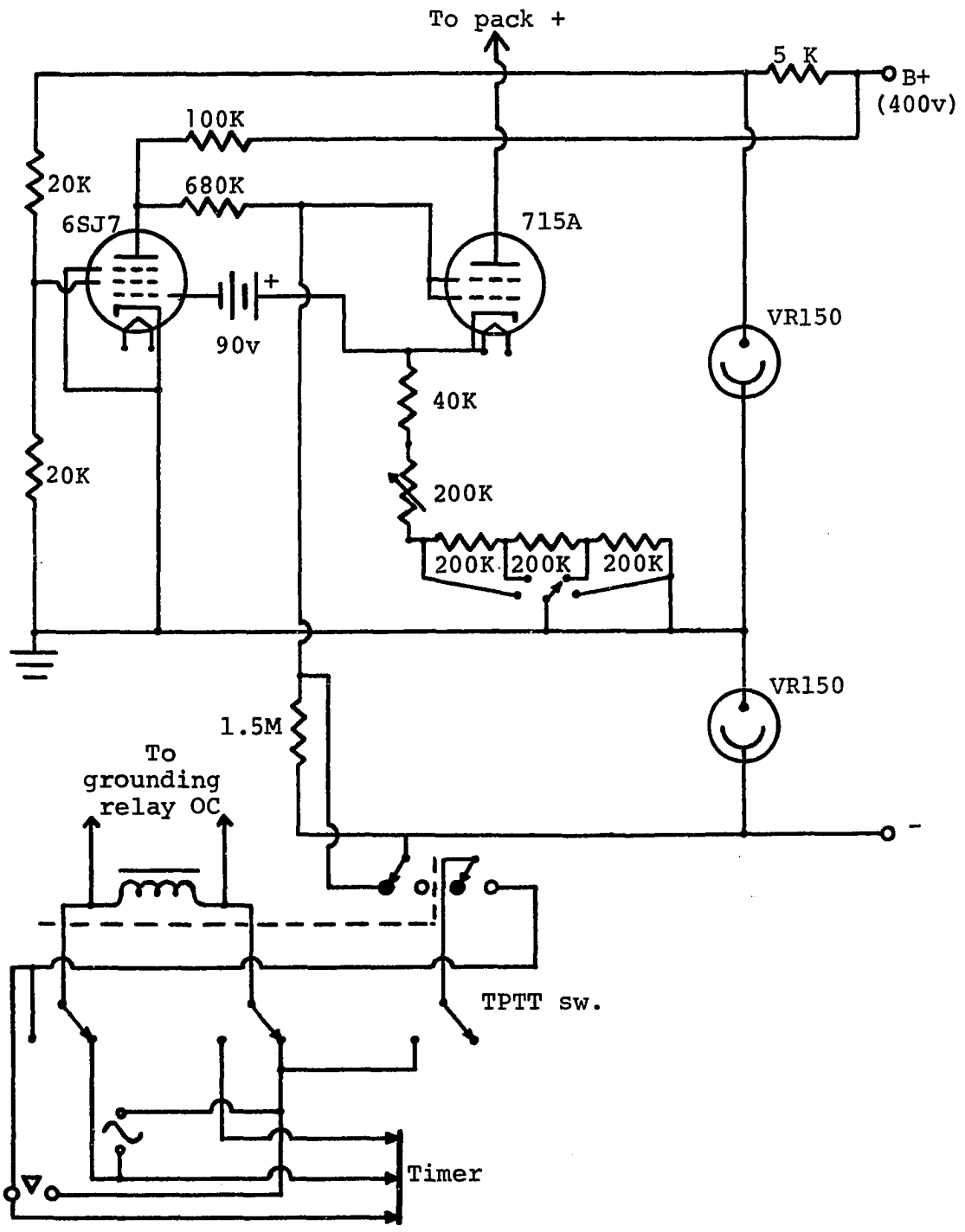


Figure 2. The Regulator Circuit.

The measurements demonstrated that secondary reactions became pronounced after about 15-20 seconds of discharge time in initially pure CO_2 , and less than 10-12 seconds in water vapor in the respective pressure ranges used. Therefore, the measurements were taken after short discharge times Δt of the order 1-12 second in a fresh filling of gas for every run.

After discharge, the remaining molecular gas (either CO_2 or H_2O vapor) was frozen out in order that the pressure of noncondensable gases formed might be measured. It was noted that as soon as the trap was cooled to the liquid nitrogen temperature, the pressure due to condensable components of the gas mixture fell quickly, and then it continued to fall at a comparatively low rate, slowly approaching a steady value. The reason for this phenomenon is that the permanent gas products formed in the volume were carried into the trap along with the condensing gas, and the pressure in the trap eventually became the same as that of the condensable and permanent gas mixture in the system. At this point no mass flow of the gas mixture into the trap was possible, and further condensation could occur only by the slow process of interdiffusion. A similar observation has been reported by Kenty⁽¹⁵⁾ in connection with the freeze-out of xenon containing a small quantity of oxygen. Sufficient time, at least about 10 minutes, therefore, had to be allowed for a thorough clean-up of the remnant CO_2 and H_2O , still the main bulk of the gas after the conclusion of a short-period discharge. Then, the pressure of the gas remaining in the system could be said to be due exclusively to the permanent gas products formed.

The measurable pressure changes were the increase in pressure after the discharge Δp and the pressure of the permanent gas products ΔP . Both Δp and ΔP were relatively small quantities of the order of tens of mTorr. To determine these quantities with good precision, proper precaution must be exercised in reading the manometer.

It is known that manometers, in general, may suffer from three major detrimental effects^(16,17). One of these is the possible contamination of the gas to be measured by absorbents in the oil; the second may arise from the contamination of the gas sample by the oil vapor, and the third is the uncertainty whether a differential displacement of the oil levels represents a true pressure or a surface tension effect. Because of a proper application of vacuum hygiene and oil of a sufficiently low vapor pressure coupled with a manometer design already described, the first two effects were believed to be reduced to an insignificant extent under the conditions of the present experiments.

The third disadvantage was circumvented in part by the employment of a micrometer eyepiece. In addition, the smooth curvature of the meniscus was illuminated such that a sharp boundary for the interface of the gas and the manometer oil could be defined after it was made certain that the meniscus was not distorted optically. Very importantly, the meniscus was always approached with the hairline in the same direction to avoid a possible backlash of the micrometer screw.

An error analysis was made of the differential pressure readings. Although the micrometer is more precise by an order of magnitude than the cathetometer scale, which can be read directly to ± 0.005 cm, it is necessary to calibrate the divisions on the micrometer drum using the cathetometer scale as a length standard.

The procedure for this calibration consisted of defining a series of lengths by the cathetometer followed by a measurement of the same lengths by the micrometer. The results were fit by least-squares technique to a straight line⁽¹⁸⁾. This analysis shows that the least micrometer division which can be directly read corresponds to $(6.644 \pm 0.017) \times 10^{-4}$ cm. Thus, the manometer displacements can be measured with an accuracy of 0.26 per cent. The precision of the pressure measurements corresponding to one division on the micrometer is ± 0.4 mTorr, the conversion factor being 0.616 Torr per cm of the oil used, at 0° C.

In this treatment the only source of error assumed is the uncertainty of the cathetometer readings in the fourth significant figure. (The standard deviation of these is determined as 0.0022 cm) Of course, there may be other sources of uncertainties, such as the occasionally improper matching of the hairline with the boundary of the meniscus. Therefore, it was estimated that with the manometry employed, the reproducibility of measurements was well within 1 mTorr.

It is also to be noted that the permanent gas measured with the manometer is enclosed in a volume which extends over two regions maintained at radically different temperatures. In the liquid-nitrogen trap of volume v_t the temperature of the permanent gas is 77°K , while the rest of the system of volume v_s contains the same gas at room temperature T . The actual pressure readings were corrected for this large temperature difference by considering that the number of gas molecules enclosed in the entire volume B of the system and having a pressure of P_1 at room temperature T must be the same as the number of molecules (determined in terms of pressure readings p_2) occupying the partial volumes v_s and v_t at temperatures T and 77°K , respectively. Accordingly, the ratio of the true pressure to the actual pressure reading is given by

$$\frac{P_1}{p_2} = \frac{77v_s + Tv_t}{77 B}, \quad (\text{II.6})$$

where $B = v_s + v_t$.

In a typical case the volume of the region cooled to the temperature of the liquid-nitrogen bath was 17 cm^3 , and the rest of the system having a volume of 806 cm^3 contained the gas at room temperature. The correction for each value of permanent gas pressure measured amounted to 5.9 per cent.

With the measurement of the pressure changes Δp and ΔP , it is possible to deduce the amount of molecular gas lost by dissociation.

If p is the pressure of the gas M admitted to the system, and p' is its partial pressure after discharge, then the pressure of the gas lost by dissociation is

$$-\Delta p(M) = p - p' . \quad (\text{II.7})$$

But, the pressure due to the remaining gas is the difference between the increased total pressure p'' after discharge and the permanent gas pressure ΔP , i.e.,

$$p' = p'' - \Delta P . \quad (\text{II.8})$$

In terms of the measured quantities,

$$p'' = p + \Delta p . \quad (\text{II.9})$$

From Eqs. (II.8) and (II.9) then

$$p' = p + \Delta p - \Delta P , \quad (\text{II.10})$$

which combined with Eq. (II.7) gives

$$-\Delta p(M) = \Delta P - \Delta p . \quad (\text{II.11})$$

This expresses the pressure of the molecules that disappear in dissociating collisions. The dissociation coefficient given in Eq. (II.5) incorporating Eq. (II.11) can now be given as

$$\frac{\alpha_d}{p_o} = 5.66 \times 10^{-3} \frac{B}{i\Delta\lambda p_o} \left(\frac{\Delta P}{\Delta t} - \frac{\Delta p}{\Delta t} \right) , \quad (\text{II.12})$$

in which all pressure measurements are reduced to 0° C.

The system volume B was determined by sharing a known quantity of gas between it and a previously evacuated bulb of known volume.

Equation (II.12) tacitly assumes that the dissociation of molecular gases leads exclusively to permanent gas products. For the gases investigated, CO₂ and H₂O vapor, this assumption will be justified when the results of observations are presented. It will be shown that, in addition to some external evidence, the assumption involved in negating the formation of condensable products is consistent with the experimental data.

The general approach to obtain the rate coefficients of dissociation expressed by Eq. (II.12) is realized by measuring the rate of disappearance of the molecules of interest, $(\Delta P - \Delta p)/\Delta t$ while maintaining a constant discharge current. The length ℓ of the positive column is varied in order to subtract the effects of the electrode regions on the reaction rate and to determine the value of E/p in the positive column corresponding to the observed dissociation rate. However, discussion of the particular ways to determine the rate of electron-impact reaction must be preceded by an examination of the behavior of the uniform positive column in the given molecular gases in order to ascertain the feasibility of observing single-collision events.

CHAPTER III

REMARKS ON THE UNIFORM POSITIVE COLUMN IN CARBON DIOXIDE AND WATER VAPOR

The positive column is that region in the complicated structure of a glow discharge which is bounded on the cathode side by the Faraday dark space and near the anode by the anode fall. The prominent characteristic of the column is that its luminosity and electrical properties are the same at various distances from the cathode. It spreads laterally to the walls filling the entire cross section of the tube at pressures of a few Torr; at higher pressures it tends to constrict radially.

In general, an equal number of electrons and ions are contained in the column per unit volume, i.e., $n_e \approx n_+$. Considering the elementary description that, if the electrons move toward the anode with an average velocity v_e , $n_e v_e$ gives the number of electrons passing through unit cross-sectional area per unit time, and $n_e v_e e$ is the electron current density, e being the electronic charge. Similarly, the ion current density is given by $n_+ v_+ e$; thus, the total current density is

$$j = (n_e v_e + n_+ v_+) e .$$

Since $n_e \approx n_+$, and the light electrons are much more mobile than the heavy positive ions, it follows that $n_e v_e \gg n_+ v_+$. Therefore, the electron current in the positive column is almost entirely carried by the electrons, as it has been noted before.

The electric field was measured by a movable anode while keeping the discharge current constant in the manner already described, and thus, measuring the extra potential necessary to sustain a short additional length of the uniform column.

It must be emphasized here that the positive columns in the gases investigated were classified uniform by visual observation only. It is to be kept in mind that the appearance of uniformity may be deceptive: rotating-mirror experiments have shown a long time ago that very rapidly moving striations with velocities of the order of 10^5 cm/sec may occur in an apparently uniform column.

The reduced field E/p is not an independent variable in the positive column of a glow discharge. This follows from the conspicuous role played by the walls of the discharge tube in determining the mechanism of the positive column. Both the electrons and ions produced by electron impact continually collide with the tube, and since they recombine there before their re-entry into the discharge volume, both cease to be carriers of current. These losses must be made up by ionizing collisions; hence, to maintain the positive column in equilibrium, the loss of charges on the wall per unit column length must equal the gain by ionization per unit column

length. The mathematical formulation of this condition (cf. the Schottky and von Engel-Steenbeck theories^(19,20)) shows that, especially at pressures of the order of 1 Torr and above, the ratio of the mean free path to the tube radius, λ/R , has a strong effect on the electric field E . Consequently, E/p is functionally dependent upon the reduced radius pR , where p is pressure and R is the tube radius.

The properties of the uniform positive column in molecular gases have not been studied as extensively as in the rare gases. Some substantial work has been done on diatomic gases, but there are no known experimental data for the axial electric field in carbon dioxide and only a little in water vapor. The reason for the lack of information became rather evident in the course of the present experiments.

In carbon dioxide at selected pressures higher than about 5 Torr, even when the discharge current was low, and at any pressure below or above 5 Torr with the current exceeding 1 mA, the discharge became highly unstable. Under these circumstances a bright violet-colored spot, apparently the negative glow from the inside of the hollow cathode, appeared quickly circling on the edges of the electrode, and often a manifest decrease in the fairly bright, milky-blue luminosity of the column occurred with a constriction setting in. These phenomena were associated with highly irregular changes in the discharge tube voltage and thus, the V vs. ℓ plots used in finding the electric field in the column were not reproducible.

As the results of the experiments will show, the electron-impact reaction, i.e., the appearance of dissociation fragments, proceeds at a fairly rapid rate, and after a short duration of the discharge (about 15-20 sec), the secondary reactions obviously exert an increasing influence on the mechanism of the discharge, so far as to upset its stability. This means that the appearance of neutral fragments in short order continuously changes the constitution of the gas, and the discharge rapidly ceases to be that in pure CO_2 .

Very similar conclusions can be drawn from the observations on the positive column in water vapor. In the case of water the current could be raised to values exceeding 1 mA without seriously disturbing the stability of the interelectrode potential. However, at pressures in the neighborhood of 5 Torr the Faraday dark space tended to occupy a considerable portion, sometimes as much as one third of the tube between the electrodes. This occurred also at lower pressures when the discharge time exceeded about 10 seconds. Simultaneously, at higher pressures a constriction of the faint bluish-white column was generally observed, and the very bright lilac-colored negative glow crept slightly outside of the cathode. At lower pressures of about 1 Torr or less, fast striations set in within less than 10 seconds and these gradually slowed down with increasing discharge time. Again, it was evident that the rapid increase in the relative concentration of the dissociation products intensified the role of secondary processes and destroyed the uniformity of the column. It is clear, then, that an investigation of

the uniform-column characteristics of a molecular gas, such as CO_2 or water vapor, cannot be carried out for the ranges of current and pressure applicable to rare gases.

It was noted in previous investigations on the positive column in water vapor⁽²⁴⁾ that it became extremely turbulent at currents of about two orders of magnitude higher than those used in the present experiments. The turbulence was accompanied by the observation of unsteady values of the pressure. Such uncertainties of pressure measurements can be, at least in part, accounted for if the extremely rapid change in the gas number density due to the rapid appearance of dissociation products is considered.

It has also been observed⁽²¹⁻²³⁾ that in oxygen at a pressure of 4 Torr a very abrupt change takes place in the electric field of the column, a jump from about 5 to $32 \text{ v}\cdot\text{cm}^{-1}$ when the current was increased from about 75 mA to 90 mA, this interval being the region in which the measurements are not reproducible.

A similar type of change in the mode of E/p was observed in the experiment with CO_2 . At a pressure of 5 Torr and with a current of 0.6 mA, the column became constricted, exhibiting irregularity in the electric field which varied between 140 and $200 \text{ v}\cdot\text{cm}^{-1}$. The stability was not regained by a change in current, and this irregularity persisted for even such short periods of discharge as 12 seconds or less. A similar instability occurred also in H_2O vapor: in approximately the same pressure range as for CO_2 , and with a

discharge current of 0.5 mA, the interelectrode potential drifted by quite large values. Although the currents employed in these experiments were over an order of magnitude less than the critical values of currents in O_2 to cause such large shifts in the field, the discharge times for CO_2 and H_2O vapor were very small. As an inspection of Eq. (II.12) reveals, the time duration of discharge and the rate of electron flow are closely linked quantities. Thus, there may not be such a great discrepancy in the comparison of the anomalies of E/p between O_2 and the molecular gases observed, CO_2 and H_2O vapor.

The regions of uncertainties as described above were carefully avoided in the experiments on both CO_2 and H_2O vapor dissociation. The observed pR dependence of E/p for CO_2 is shown in Fig. 3, for H_2O vapor in Fig. 4. The shape of these curves are similar to those for the rare gases and some molecular gases such as H_2 and N_2 . The graphs indicate the range of E/p useful for the dissociation experiments. They also provide an assurance that the positive columns of CO_2 and H_2O vapor discharge were indeed uniform and allowed single-event observations.

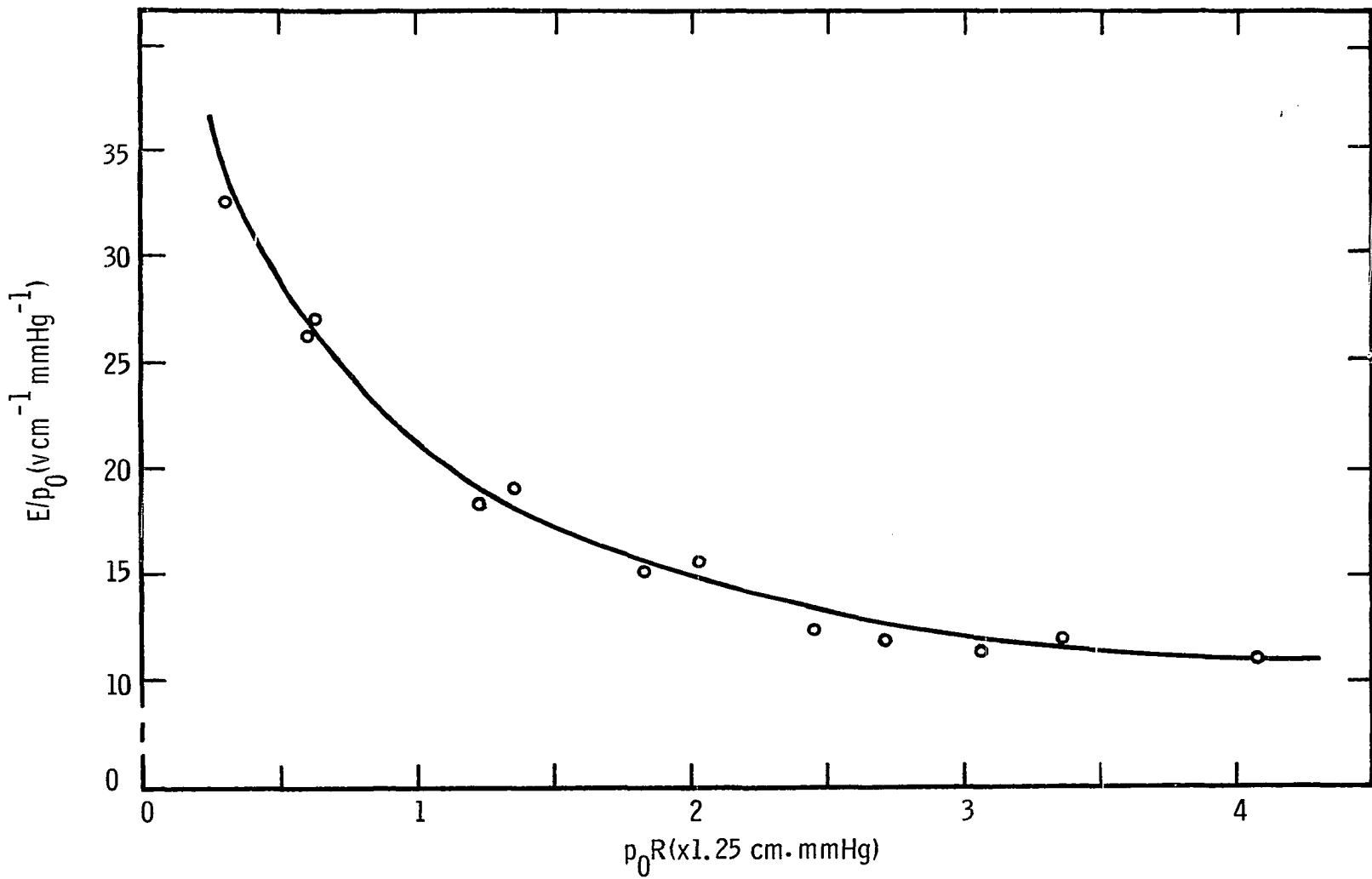


FIGURE 3. The Dependence of E/p on pR for CO_2 Measured at a Discharge Current of 0.6 mA and a Tube Radius of 1.25 cm.

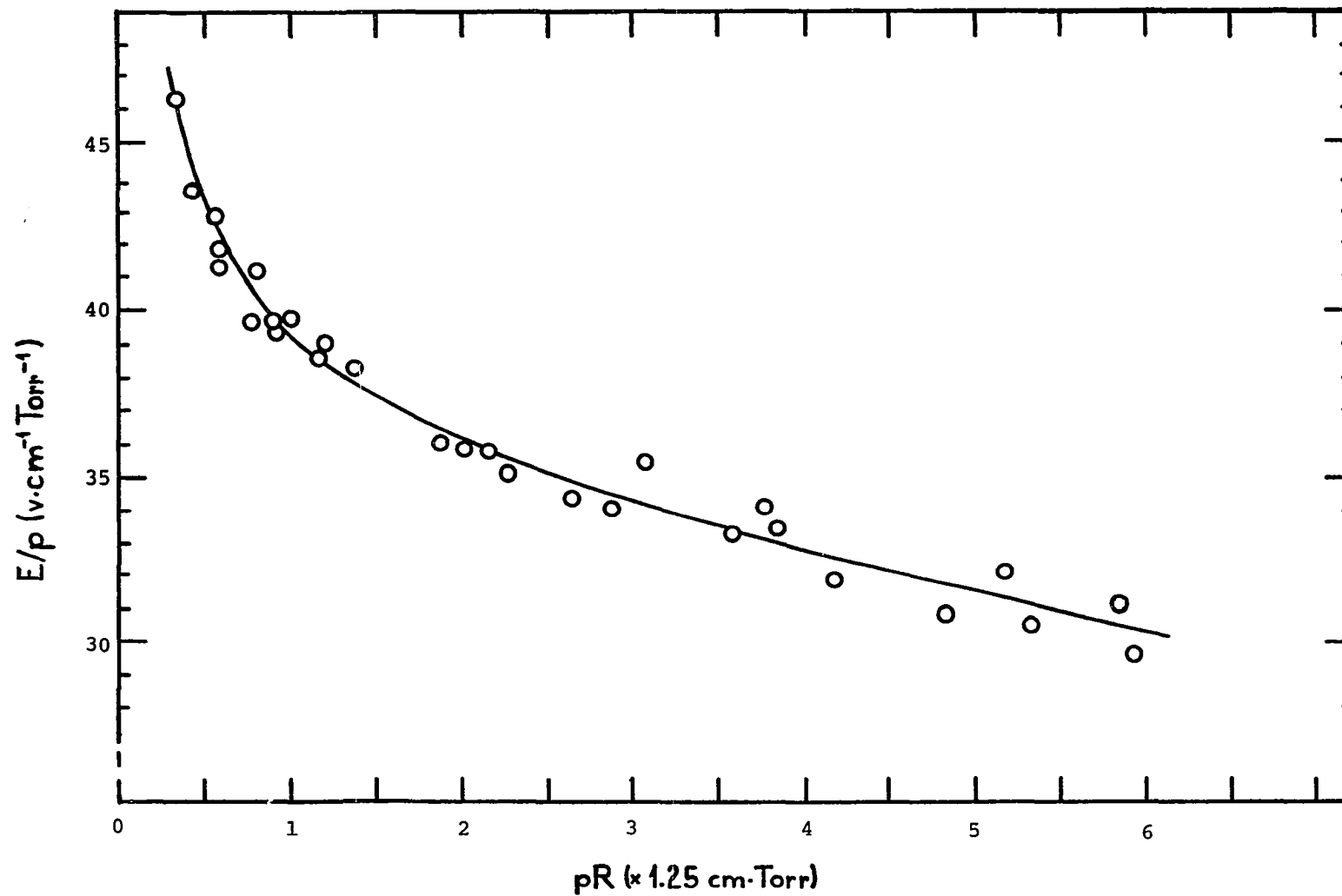


FIGURE 4. The Dependence of E/p on pR for H_2O Vapor at Discharge Currents Between 0.3 and 0.7 mA and a Tube Radius of 1.25 cm.

CHAPTER IV

PRESENTATION AND DISCUSSION OF RESULTS

As an initial step, the variations after discharge in the observed pressure increase Δp and the pressure due to the permanent gas ΔP were measured with respect to the time duration of the discharge t . These measurements were repeated for various values of E/p . Hence, the observations of the time rates of change of the increase in the differential pressures, which were produced by discharges lasting sufficiently short intervals in fresh samples of gases, constituted the major and most systematic approach to an experimental determination of the rate coefficients of dissociation for both CO_2 and H_2O vapor.

Another approach leading to a measurement of rate coefficient is offered by Eq. (II.11) which gives the number of molecules disappearing in dissociating collisions as the difference between the pressure of the permanent gas products and that due to the increase in the initial pressure of the sample after discharge. Consequently, it is possible to observe the rate of molecular dissociation at selected lengths of the positive column and, in turn, to deduce the rate coefficients by means of Eq. (II.12). However, this method is, in general,

severely handicapped by phenomena associated with the absorption of gases to the walls of the discharge tube; namely, the irregular desorption sometimes may introduce large random errors into the measurements of Δp and thus, increase the uncertainty in the values of dissociation coefficients.

Despite its disadvantage, the latter method has not been discarded since, as examples will show in the following paragraphs, it can be useful if one has already established the measurements showing the time-dependence of differential pressure changes.

The Rate Coefficient of Dissociation for CO₂

The characteristic time dependence of the pressure changes Δp and ΔP in CO₂ is shown by Figs. 5 and 6. It is seen on these graphs that there is a region over which both Δp and ΔP increase linearly with time. For longer time, the pressure changes become nonlinear, presumably due to the increasing effect of reverse reaction which reforms CO₂ from the accumulated dissociation products. The curves for Δp , the pressure rise after discharge, indicate that there is evidence for an initial nonlinear pressure increment which causes the extrapolation of the linear part of the graph to make a finite positive intercept at zero time.

This behavior must be attributed to a rapid initial production of a condensable gas when the discharge is switched on. The initial increment cannot be due to a permanent gas since if this were the case,

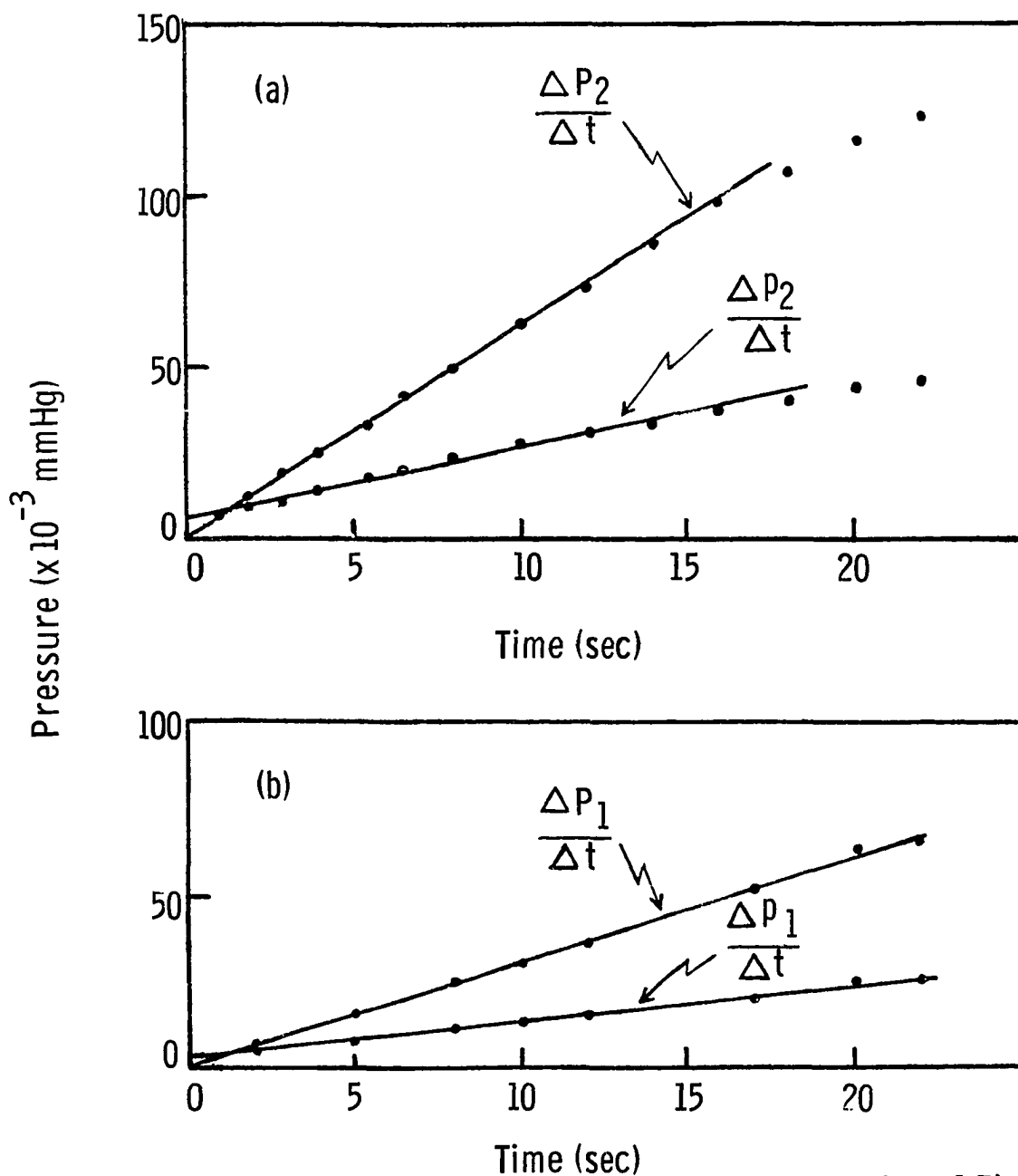


FIGURE 5. The Pressure Changes ΔP and Δp Plotted as a Function of Time for $p_0 = 1.23$ Torr of CO_2 , at $i = 0.6$ mA and an E/p of $18.6 \text{ v} \cdot \text{cm}^{-1} \cdot \text{Torr}^{-1}$.
 (a) $l_2 = 70$ cm, (b) $l_1 = 30$ cm.

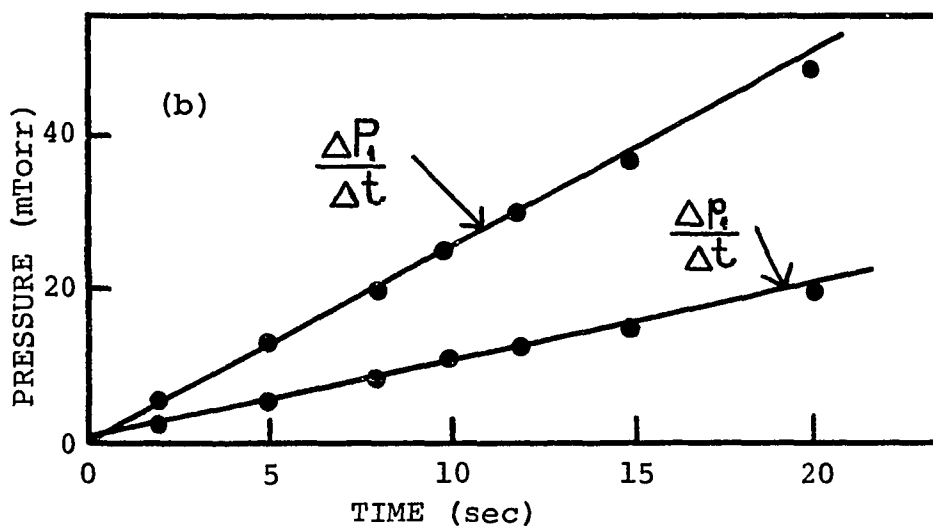
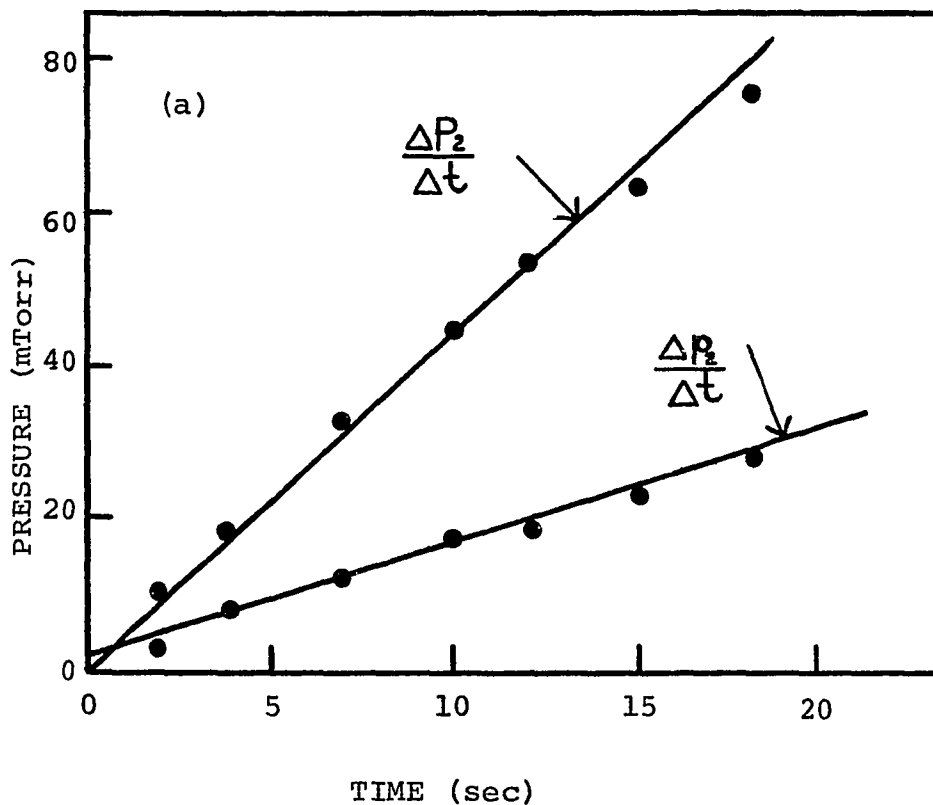


FIGURE 6. The Pressure Changes ΔP and Δp Plotted as a Function of Time for $p_0 = 3.08$ Torr of CO_2 and $i = 0.6$ mA, $E/p_0 = 11.2$ v·cm·lTorr⁻¹. (a) $l_2 = 40$ cm, (b) $l_1 = 20$ cm.

a similar nonzero intercept would be found for the ΔP curves. It may be assumed that CO_2 is partially liberated from the tube walls when the discharge is first switched on. This uncertainty due to desorption is removed by considering only the slopes of the linear portion of the curves.

With the discharge current constant at 0.6 mA, the time rates of change of Δp and ΔP were measured for two different electrode separations, l_1 and l_2 . Then, the difference of the slopes of the ΔP and Δp lines obtained with discharge path lengths l_2 and l_1 , respectively, gave the amount of pressure change caused by a length $(l_2 - l_1)$ of positive column, at a particular value of E/p_0 .

The slopes $\Delta P/\Delta t$ and $\Delta p/\Delta t$ determined in this manner are listed in Table 1 where the subscripts 1 and 2 refer to measurements taken at two different lengths, l_1 and l_2 , of the positive column. On the basis of these data it is now possible to write the dissociation coefficient of CO_2 , given in Eq. (II.12), as

$$\frac{\alpha_d}{p_0} = \frac{k}{(l_2 - l_1)p_0} \left[\left(\frac{\Delta P_2}{\Delta t} - \frac{\Delta p_2}{\Delta t} \right) - \left(\frac{\Delta P_1}{\Delta t} - \frac{\Delta p_1}{\Delta t} \right) \right], \quad (\text{IV.1})$$

in which the numerical factor k , 5.66×10^{-3} B/i, is 7.76×10^3 for a discharge current of 0.6 mA and system volume B of 823 cm^3 used in these measurements.

Table 1. Dissociation coefficients for carbon dioxide from the observations on the rates of increase of non-condensable dissociation products in a segment Δl of the positive column.

P_0 (Torr)	0.31	1.23	3.08
Δl (cm)	40	40	20
$\frac{\Delta P_2}{\Delta t}$ (mTorr/sec)	4.98	6.11	4.57
$\frac{\Delta p_2}{\Delta t}$ (mTorr/sec)	1.69	2.00	1.57
$\frac{\Delta P_1}{\Delta t}$ (mTorr/sec)	3.49	3.05	2.72
$\frac{\Delta p_1}{\Delta t}$ (mTorr/sec)	1.27	1.03	0.93
$\frac{B}{i p_0}$ ($\times 10^5 \text{ cm}^3 \cdot \text{amp}^{-1} \cdot \text{Torr}^{-1}$)	44.5	11.1	4.4
E/p_0 ($\text{v} \cdot \text{cm}^{-1} \cdot \text{Torr}^{-1}$)	32.5	18.6	11.2
α_d/p_0 ($\text{electron}^{-1} \cdot \text{cm}^{-1} \cdot \text{Torr}^{-1}$)	0.67	0.33	0.15

It is evident from the data of Table 1 and the complementary Figs. 5 and 6 that the ratio of the slopes, the time rate of appearance of permanent gas products $\Delta P/\Delta t$ and that of the increase in the pressure after discharge $\Delta p/\Delta t$, in all cases is closely 3:1. In addition to the significance of this fact in determining a plausible reaction mechanism for CO_2 , it is now made possible to write Eq.

(IV.1) as

$$\frac{\alpha_d}{p_0} = \frac{2}{3} \frac{k}{(\lambda_2 - \lambda_1)p_0} \left(\frac{\Delta P_2}{\Delta t} - \frac{\Delta P_1}{\Delta t} \right) \quad (\text{IV.2})$$

Since the ΔP vs. Δt and the Δp vs. Δt plots provide as precise a way to measure the dissociation coefficients as the given experimental conditions allow, these measurements can be said to define the trend by which the coefficients change with respect to E/p .

When changes in the number of molecules are measured (cf. Eq. II.11) in a given time interval, and if the values of $\Delta(\text{CO}_2)/\Delta t$ are plotted against the respective discharge paths λ , the resulting graphical display may sometimes be so disarrayed that a reasonably accurate determination of the slope, $\Delta(\text{CO}_2)/\Delta t \Delta \lambda$, is not possible. The reason for this, as it has been stated above, is that the desorption from the wall makes the readings of Δp rather erratic.

An example for a measurement of this type is given in Fig. 7. The slope, determined as $5.4 \times 10^{-5} \text{ Torr} \cdot \text{cm}^{-1} \cdot \text{sec}^{-1}$, is substituted into Eq. (II.12) now expressed as

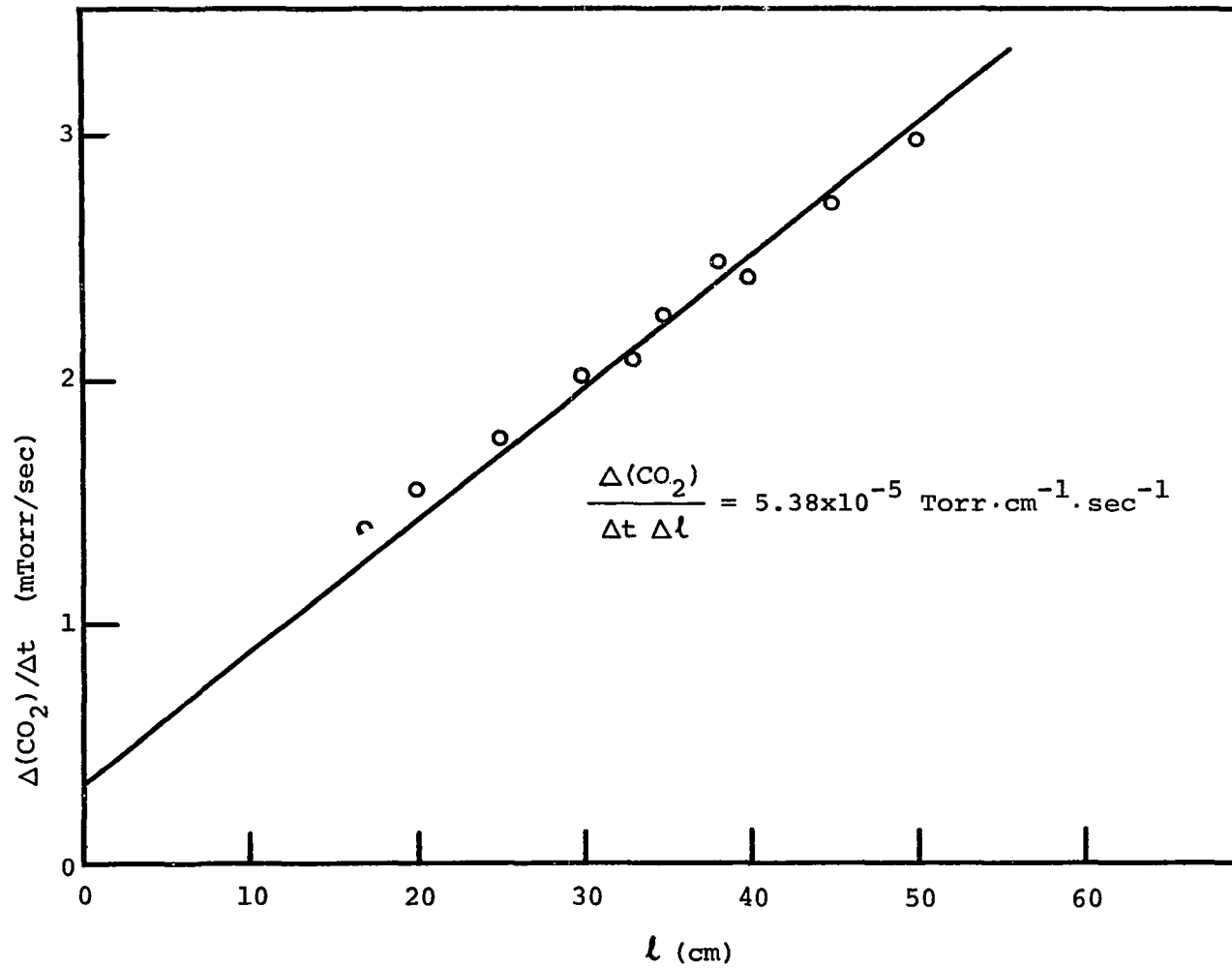


FIGURE 7. The Rate of Disappearance of CO_2 Molecules Due to Dissociation as a Function of Positive Column Length for $p_0 = 2.06$ Torr and $i = 0.6$ mA.

$$\frac{\alpha_d}{p_0} = 5.66 \times 10^{-3} \frac{B}{ip_0} \frac{\Delta(CO_2)}{\Delta t \Delta \ell} , \quad (IV.3)$$

yields a rate coefficient of 0.23 at E/p of 15.8. If in the measurements for $\Delta(CO_2)$ the values of Δp are ignored and only the data for $\Delta P/\Delta t$ are used in calculating the dissociation coefficients, then Eq. (IV.2) can be applied in the form

$$\frac{\alpha_d}{p_0} = \frac{2}{3} \frac{5.66 \times 10^{-3} B}{ip_0} \frac{\Delta P}{\Delta \ell \Delta t} . \quad (IV.4)$$

The data indicated in Fig. 7 gives, by means of Eq. (IV.4), a rate coefficient of 0.26 from which the previously calculated value deviates by about 15 per cent.

The example chosen may be fortuitous since in some cases such a deviation may amount to as much as 40 per cent. Nevertheless, $\Delta P/\Delta t$ vs. ℓ plots can be used successfully in determining the (E/p) -dependent values of dissociation coefficients provided that measurements of the type shown in Figs. 5 and 6 are clearly established beforehand. Then, the method implied in Eq. (IV.3) can be made to conform with the one expressed by Eq. (IV.1). Measurements that have been brought in accord in such a fashion with the type of measurements indicated in Table 1 are given in Table 2.

As a summary of all the results obtained, the dissociation coefficient α_d/p_0 is shown as a function of E/p_0 in Fig. 8. The coefficients were all measured at a current of 0.6 mA, but some of the

Table 2. Dissociation coefficients for carbon dioxide obtained by measuring the changes in $\Delta(\text{CO}_2)/\Delta t$ with respect to ℓ , and subsequently recalculated by considering the rates of appearance of permanent gas products only and using Eq. (IV.4).

P_0 (Torr)	0.62	0.67	1.39	1.85	2.06	2.46	2.72	3.38	4.41
Slope of $\Delta(\text{CO}_2)/\Delta t$ vs. ℓ plots ($\times 10^{-5}$ Torr $\cdot\text{cm}^{-1}\cdot\text{sec}^{-1}$)	3.1	4.5	7.8	4.8	5.4	5.0	4.6	4.7	4.7
α_d/p_0 (From $\Delta(\text{CO}_2)/\Delta t$ vs. ℓ)	0.39	0.60	0.48	0.20	0.23	0.16	0.15	0.12	0.10
B/ip_0 ($\times 10^5$ cm $^3\cdot\text{amp}^{-1}\cdot\text{Torr}^{-1}$)	22.1	23.4	11.3	7.4	7.6	5.6	5.7	4.6	3.8
$\Delta P/\Delta t \Delta \ell$ ($\times 10^{-5}$ Torr $\cdot\text{sec}^{-1}\cdot\text{cm}^{-1}$)	6.7	7.3	10.1	9.3	9.2	7.5	6.9	9.8	11.3
E/p_0 (v $\cdot\text{cm}^{-1}\cdot\text{Torr}^{-1}$)	25.8	29.2	19.4	15	15.8	12.2	12.5	11.8	12.2
α_d/p_0 by Eq. (IV.4) (electron $^{-1}\cdot\text{cm}^{-1}\cdot\text{Torr}^{-1}$)	0.52	0.65	0.43	0.26	0.27	0.16	0.15	0.17	0.16

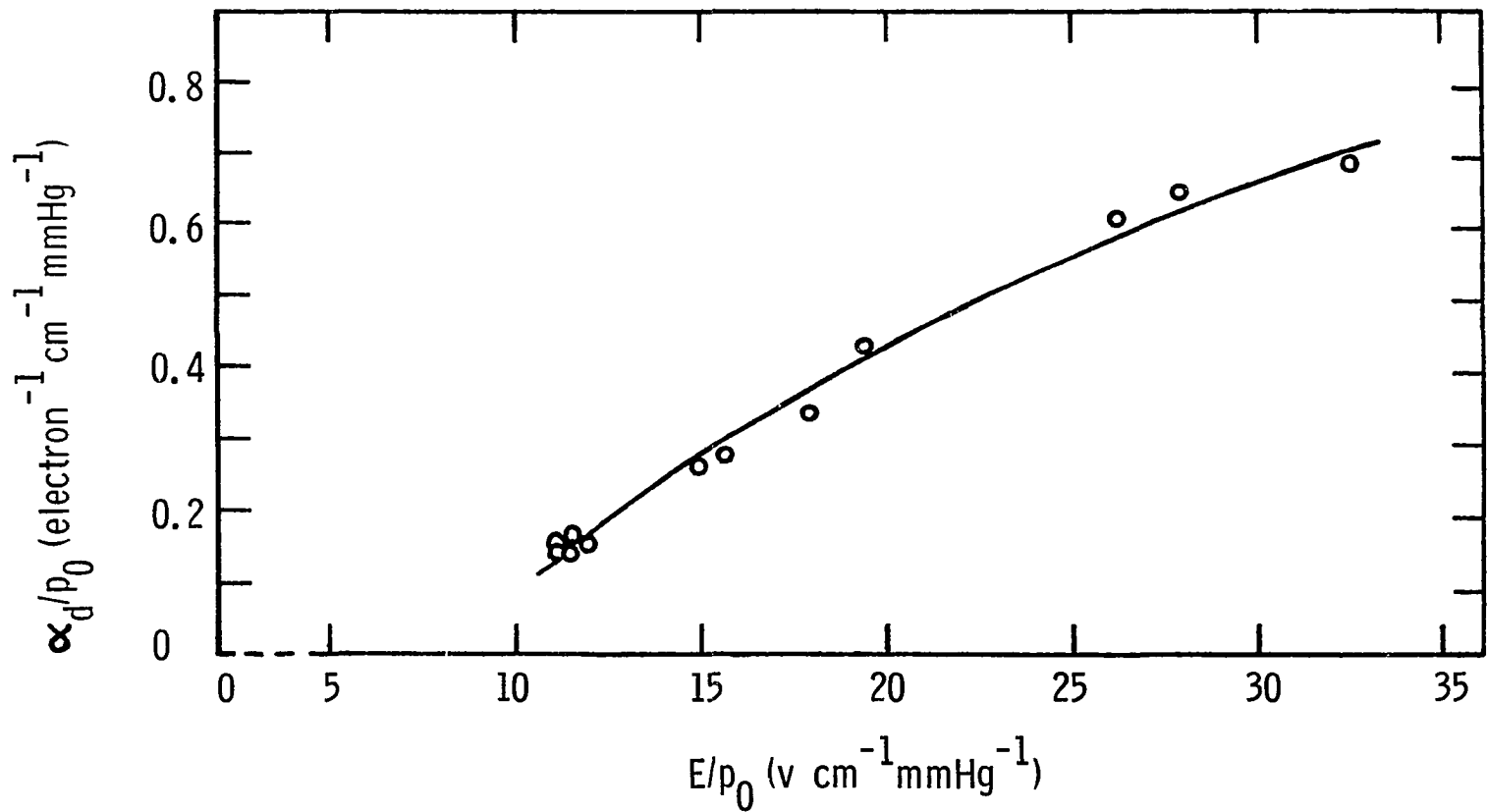


FIGURE 8. The Rate Coefficient of Dissociation for CO₂ as a Function of E/p₀.

measurements were repeated at 0.3 mA. For example, the measurements listed in the second column of Table 1 were reproduced at half values of currents. The value of $(\Delta P/\Delta l \Delta t)$ in this case turned out to be $0.4 \times 10^{-4} \text{ Torr} \cdot \text{sec}^{-1} \cdot \text{cm}^{-1}$ which led to a dissociation coefficient of 0.33, the same as that obtained at a current of 0.6 mA.

Measurements of dissociation coefficients at various currents disclosed no current dependence of these coefficients. Therefore, it was verified that dissociation proceeds by single encounter between electrons and molecules.

Dissociation Mechanism for CO₂

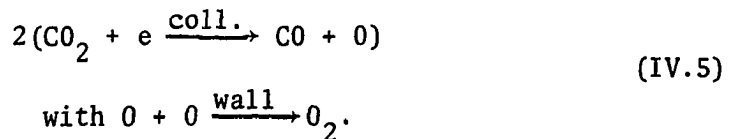
As an inspection of the slopes given in Table 1 reveals, $\Delta P/\Delta t$ and $\Delta p/\Delta t$ determined under the same conditions are very closely in the ratio 3:1. This observation enables one to deduce a plausible dissociation mechanism.

The 3:1 ratio observed implies that for every two CO₂ molecules lost by dissociation, three permanent gas molecules are formed from the dissociation products since in this way the dissociation of two CO₂ molecules gives a net increase of one in the total number of molecules present.

Carbon dioxide is a linear molecule with the carbon atom at the center. Therefore, it seems natural to assume that dissociation proceeds to give CO and O, not necessarily in their ground states, CO is, of course, a noncondensable gas, and atomic oxygen might be expected to recombine on the walls of the vessel to form O₂. Considering

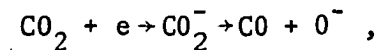
the structure of O-C-O, it seems unlikely that free carbon is formed by a single electron impact. This supposition is also supported by the fact that no free carbon is deposited in the discharge tube at any time. Hence, the evidence established in the course of the experiments bears out the *a priori* assumption involved in the derivation of Eq. (II.12): the dissociation of CO₂ indeed seems to result in permanent gas products.

If the dissociation products are carbon monoxide and atomic oxygen, then the following reaction scheme explains the observed 3:1 pressure ratios:



By this mechanism, the composition of the permanent gas produced by the dissociation of CO₂ in the positive column of the glow discharge is expected to be two molar parts of CO and one of O₂. Thus, dissociation into CO and O seems to be a plausible route for at least the bulk of the observed reaction.

Another conceivable route for the electron-impact reaction described in (IV.5) could be dissociative attachment, i.e.,



for which the cross sections have been measured by Schulz⁽²⁵⁾ and Rapp and Briglia⁽²⁶⁾. The total cross section for negative-ion formation, according to the data of Rapp and Briglia, shows two peaks in the energy range below 10 eV. The cross section with an onset of about 3.3 eV is rising to a maximum of $1.5 \times 10^{-19} \text{ cm}^2$ at 4.3 eV followed by a decrease to essentially zero at 5.8 eV; then it is rising again to another maximum of about $4.3 \times 10^{-19} \text{ cm}^2$ at 8.1 eV, reaching zero at approximately 10 eV.

This cross section was used to calculate the rate coefficient for dissociative attachment in CO_2 by the technique of estimation to be described in the following chapter. A Maxwellian distribution of electron energies has been assumed in this calculation, and the resulting coefficient for dissociative attachment as a function of E/p is shown in Fig. 9. A comparison between this curve and the dissociation coefficients displayed in Fig. 8 reveals that the coefficients for attachment are about two orders of magnitude smaller than those for neutral dissociation. In view of this fact, the role of dissociative attachment of CO_2 in the positive column must be judged as negligibly small.

The Townsend ionization coefficients measured by Young⁽²⁷⁾ are also shown in Fig. 9. These differ from the values of dissociation coefficients by the same order of magnitude as the attachment coefficients. Therefore, it follows that the electron-impact dissociation of CO_2 , for all practical purposes, must take place by way of uncharged species.

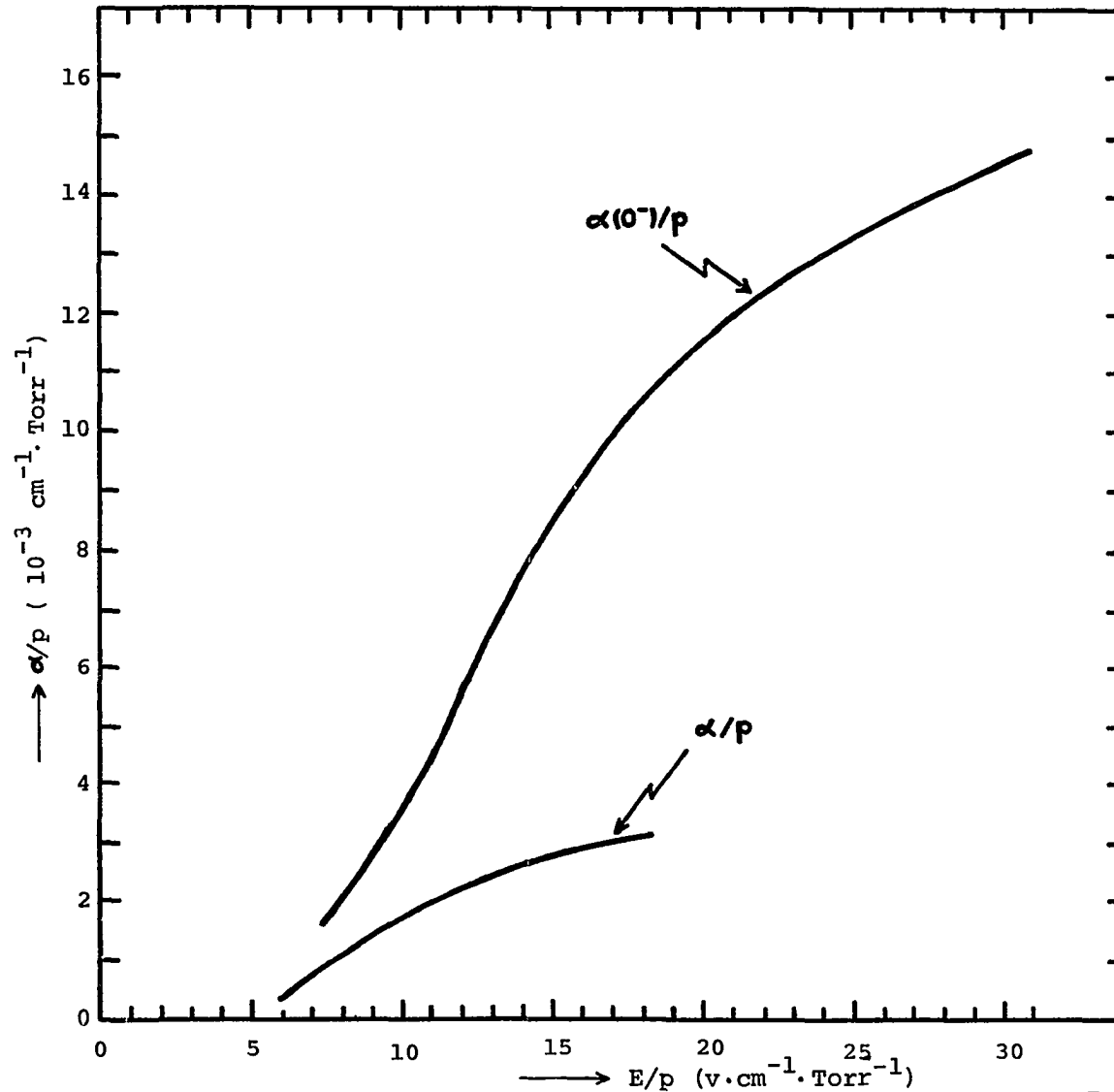


FIGURE 9. The Rate Coefficient for Dissociative Attachment in CO_2 $\alpha(O^-)/p$ Calculated from the Cross Sections Measured by Rapp and Briglia. The Lower Curve Shows Young's Data for the First Townsend Coefficient of Ionization in CO_2 α/p .

The Rate Coefficients for H₂O Vapor

When measurements of the dissociation rates in water vapor were at first attempted by the same methods of procedure as those employed for carbon dioxide, it became obvious that the pressure increments Δp appearing after discharge under the same conditions could not be reproduced precisely. The difficulties were caused by the adsorption of water vapor on the walls of the discharge tube.

It is well known that water vapor forms a multilayer on surfaces⁽²⁸⁾, and not surprisingly, adsorption takes place at rates high enough to seriously hinder accurate readings of differential pressures, especially when a sample of water is admitted to a previously evacuated system. It was, therefore, necessary to examine the adsorption rates in the pressure range of interest (0.3 to 5 Torr), at least in a cursory fashion.

Measurements were made of the time rates of disappearance of water molecules from the vapor phase before the discharge was switched on and at various initial pressures of water vapor. An example of this type of observation is given in Fig. 10, which shows the decrease of pressure of a sample, originally at about 1.9 Torr, with respect to time. This graph indicates that during the first 10 minutes adsorption proceeds at a quite high rate, and then with increasing time the pressure decrease gradually diminishes and approaches a saturation value, but certainly not reaching it within 90

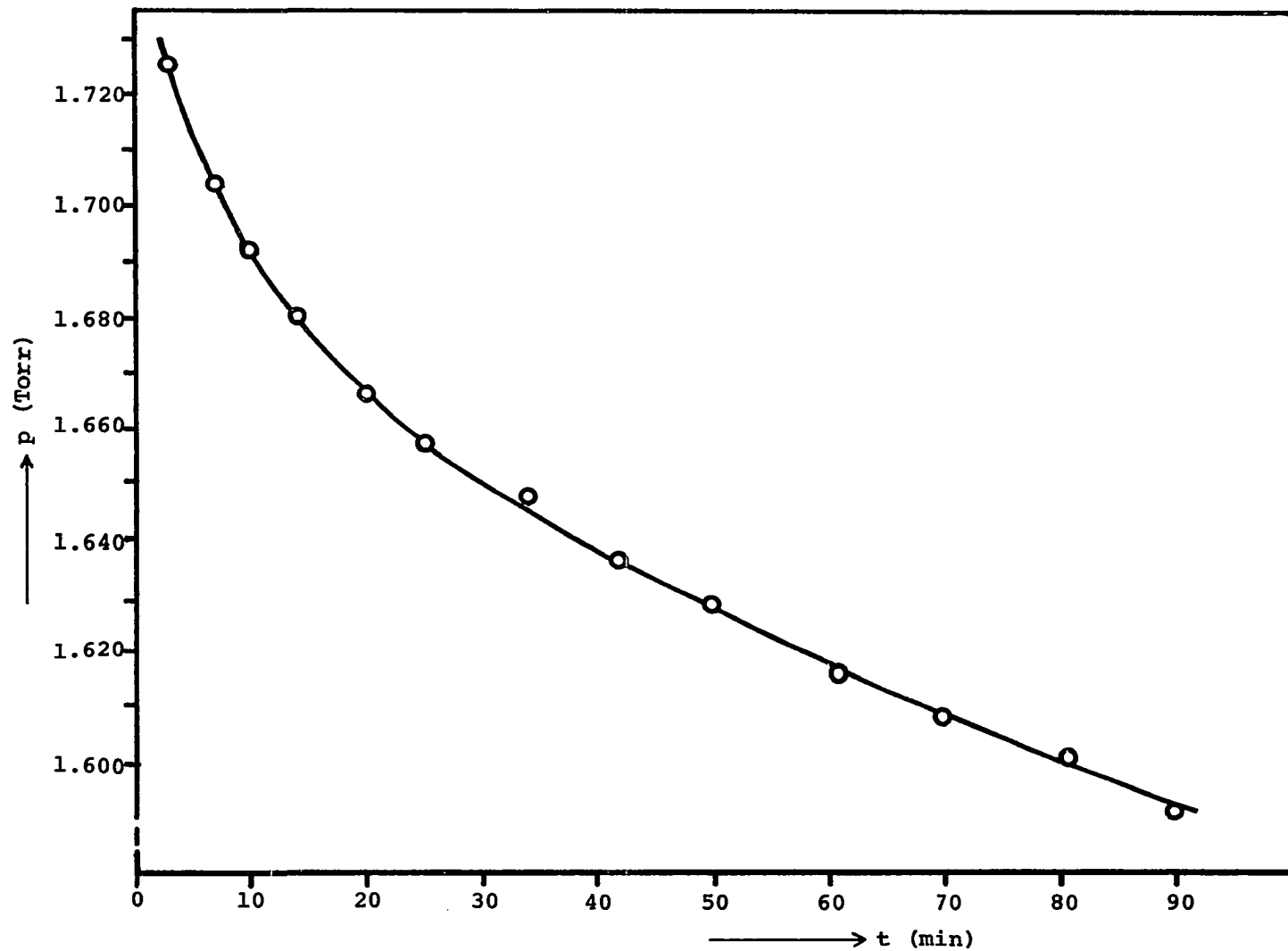


FIGURE 10. An Example Showing the Rate of Adsorption of Water Vapor in the Discharge Vessel at 25°C.

minutes. Adsorption equilibrium in no case was established within this time interval for samples in the investigated pressure range.

These measurements are summed up in Fig. 11. The two curves in this figure show the adsorption rates - $\delta P/\delta t$ plotted against the values of pressure at which the disappearance of molecules due to adsorption was observed. Graph (a) indicates rates over the interval between 5 and 10 minutes as a function of pressure averaged over that interval obtained by linear approximation. An approximation over an interval exceeding 1 minute cannot be made immediately after the introduction of water vapor into the evacuated vessel because of the extremely rapid rate of adsorption generally up to the end of the first 5-minute period. Curve (b) shows a similar kind of display for the adsorption rates determined for large intervals beginning after about 30 to 50 minutes. In this case the rate of decrease of water molecules is less than 2 mTorr/min, whereas in the first few minutes it is more than 8 mTorr/min for most of the pressure values to be used in the dissociation experiment. Curve (b) of Fig. 11, hence, serves as a guide to find how long the walls of the discharge tube will have to be exposed to the water vapor before the discharge can be switched on and before the readings of Δp appearing after discharge can be reproduced.

The measurements given in Fig. 11 were taken at 25° C with an occasional deviation of $\pm 1.5^\circ$ C; the water vapor was admitted to a system volume of 810 cm³, with a surface exposed to the vapor having

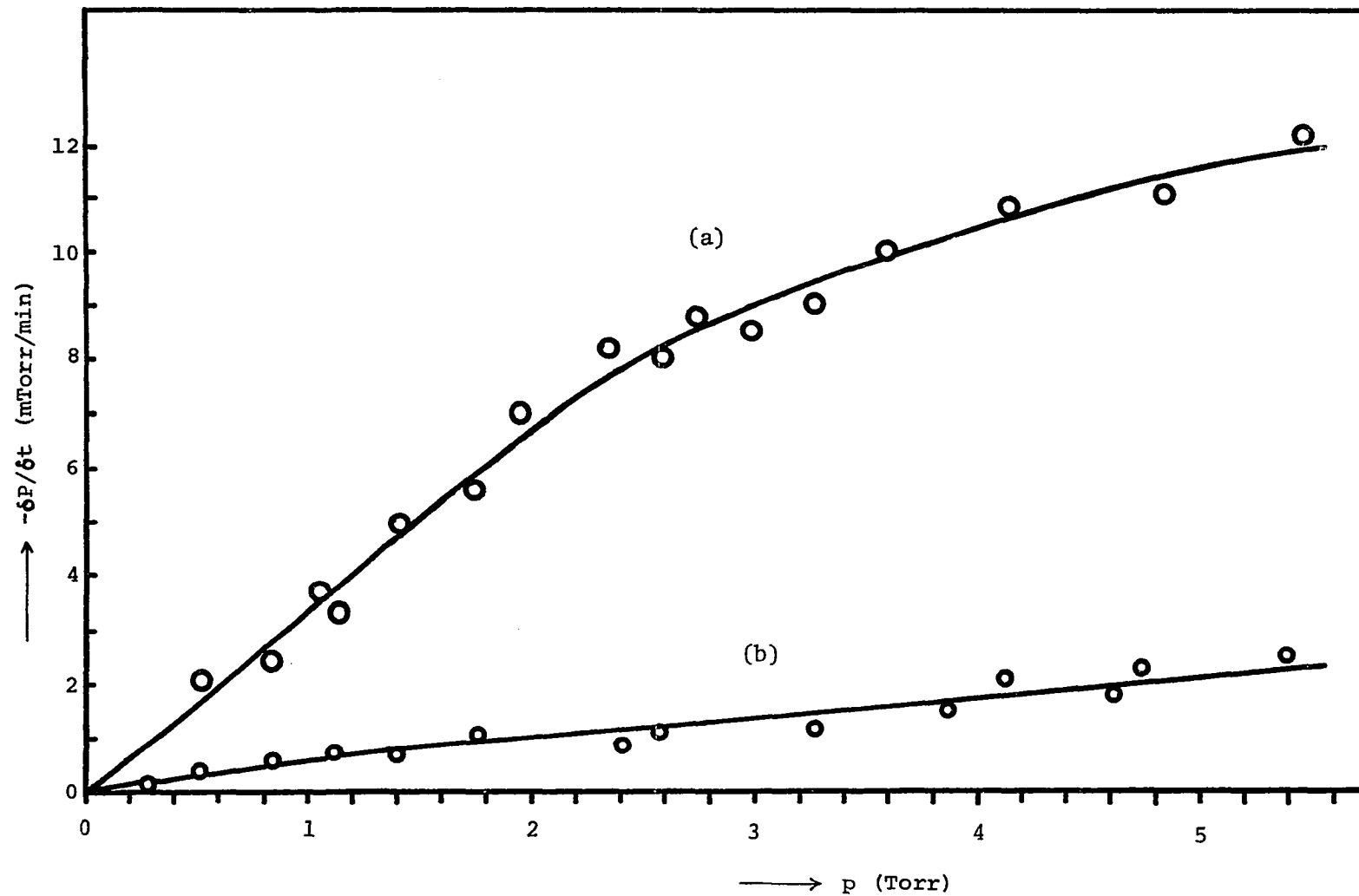


FIGURE 11. The Adsorption Rate $-\delta P / \delta t$ Plotted Against the Pressure Averaged Over the Corresponding Time Interval.

an estimated area of $1.85 \times 10^3 \text{ cm}^2$. This area was, neglecting the relatively small metallic surfaces of the electrodes, that of pyrex glass.

With the precautionary measures implied in these sufficiently quantitative observations on adsorption phenomena, such conditions were established that essentially the same procedure could be followed in measuring a dissociation coefficient as for CO_2 . The H_2O samples entering the system were allowed to approach an equilibrium of adsorption such that Δp could be determined with an adequate accuracy.

The time rates of change of Δp and ΔP were measured at two selected lengths of the positive column and a current of 0.5 mA. As before, only the linear portion of these curves were considered. These measurements are illustrated in Figs. 12 and 13. Again, the nonzero intercept of the Δp vs. t plots can be attributed to desorption of the walls as a result of bombardment by charged particles. These curves again become nonlinear at increasing times of discharge, but the change in this case is markedly different from the behavior of ΔP vs. t and Δp vs. t plots for CO_2 : $\Delta P/\Delta t$ and $\Delta p/\Delta t$ in the CO_2 column decreased with increasing time, in H_2O these rates tend to scatter rather widely about the initially quite well-defined slope. This erratic behavior in the appearance of dissociation products after discharge times of about 10-12 seconds is clearly associated with the increasing influence of secondary processes.

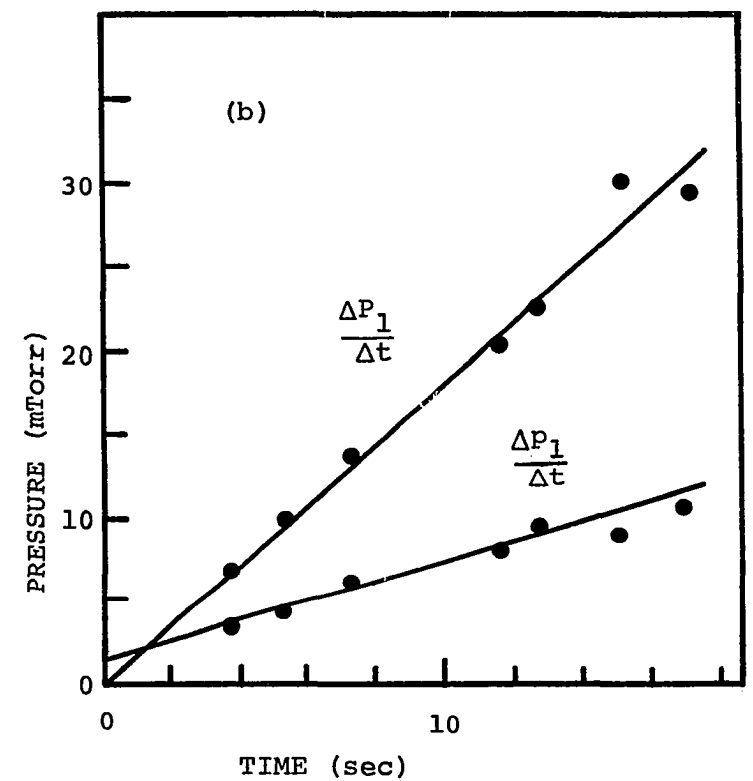
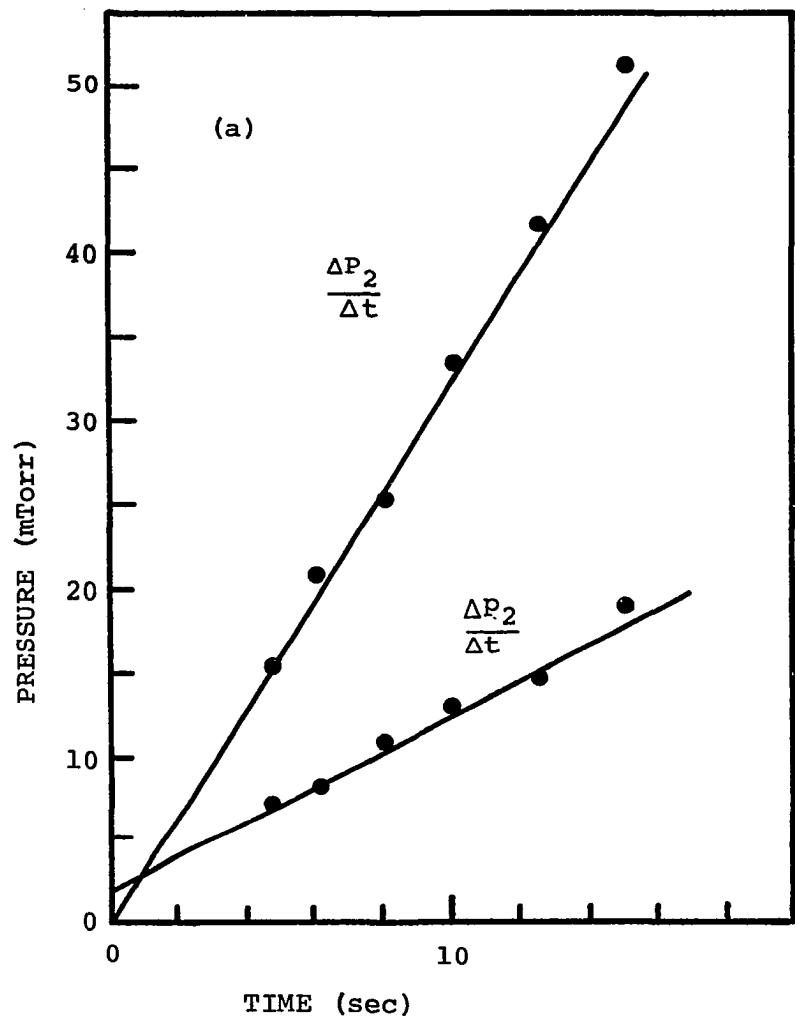


FIGURE 12. The Time Rate of Change of ΔP and Δp for 0.54 Torr of Water Vapor at a Current of 0.5 mA and an E/p of $42 \text{ v} \cdot \text{cm}^{-1} \cdot \text{Torr}^{-1}$. (a) $l_2 = 55 \text{ cm}$, (b) $l_1 = 30 \text{ cm}$.

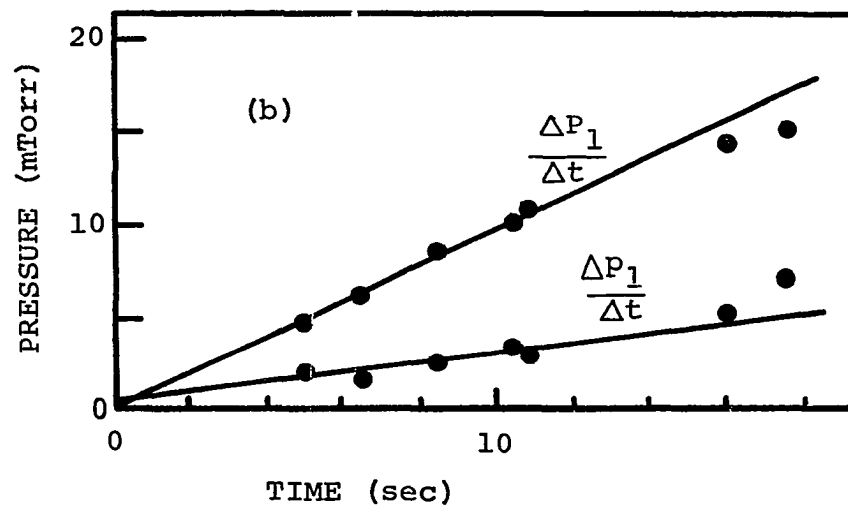
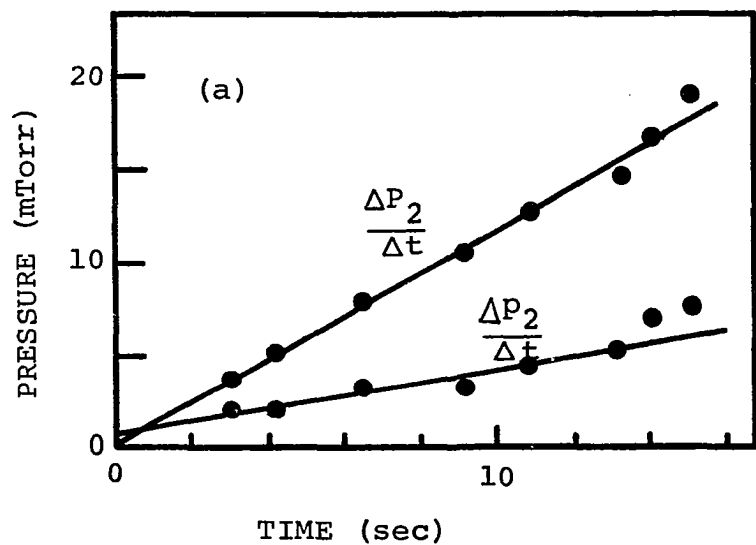


FIGURE 13. The Time Rate of Change of ΔP and Δp for 3.08 Torr of H_2O Vapor at an E/p of $35.7 \text{ v}\cdot\text{cm}^{-1}\cdot\text{Torr}^{-1}$. (a) $l_2 = 25 \text{ cm}$, (b) $l_1 = 15 \text{ cm}$.

Values for the slopes $\Delta P/\Delta t$ and $\Delta p/\Delta t$ measured at different column lengths and under the same conditions are recorded in Table 3. The ratio of slopes, $(\Delta P/\Delta t):(\Delta p/\Delta t)$, as evident from Figs. 12 and 13, are closely in the ratio 3:1 for all the measurements shown in Table 3.

The rate coefficients were calculated by means of Eq. (IV.1). It must be noted that the measurements taken were not reduced to zero for H_2O vapor. Since the number density of molecules is given by $N = n_0(p/760)(273/T)$, the equivalent density at $298^\circ K$ is $3.24 \times 10^{16} p$. Then,

$$\frac{E}{P} = 3.24 \times 10^{16} \frac{E}{N} .$$

(The equivalent density at $0^\circ C$ is $3.54 \times 10^{16} p$.) As a consequence, the numerical factor k in Eq. (IV.1) becomes $5.19 \times 10^{-3} B/i$.

The rate coefficients of Table 3 clearly establish a sequence of E/p -dependent values which, as it has been the case for CO_2 , can serve as a standard when other methods are employed in finding the dissociation coefficients. The procedure implied in Eq. (II.11) was attempted again: the number of H_2O molecules dissociated by electron impact in a given time were plotted against the corresponding discharge path lengths. The slopes of these curves allowed calculations of dissociation coefficients from Eq. (IV.3). Measurements of this type are shown in Table 4.

Table 3. Dissociation coefficients for water vapor obtained from the observed rates of increase of permanent gas products in a segment Δl of the positive column.

P (Torr)	0.44	0.54	0.90	1.19	3.08	3.77
$\frac{\Delta P_2}{\Delta t}$ (mTorr/sec)	3.50	3.25	2.60	2.10	1.18	1.05
$\frac{\Delta p_2}{\Delta t}$ (mTorr/sec)	1.23	1.05	0.90	0.75	0.38	0.325
$\frac{\Delta P_1}{\Delta t}$ (mTorr/sec)	2.00	1.83	1.20	1.30	0.97	0.95
$\frac{\Delta p_1}{\Delta t}$ (mTorr/sec)	0.75	0.55	0.38	0.40	0.34	0.32
B/ip ($\times 10^5 \text{ cm}^3 \cdot \text{amp}^{-1} \cdot \text{Torr}^{-1}$)	36.8	30.0	18.0	13.6	5.3	4.3
Δl (cm)	30	25	20	15	10	5
E/p ($\text{v} \cdot \text{cm}^{-1} \cdot \text{Torr}^{-1}$)	43.6	41.9	39.7	38.6	35.7	34.0
α_d/p ($\text{electron}^{-1} \cdot \text{cm}^{-1} \cdot \text{Torr}^{-1}$)	0.65	0.57	0.41	0.21	0.04	0.04

Since the ratio of slopes $(\Delta P/\Delta t):(\Delta p/\Delta t)$ determined under the same conditions is consistently close to 3:1 (cf. Figs. 12 and 13, and Table 3), Eq. (IV.2) can again be applied in computing the dissociation coefficient at a given value of E/p . Dissociation coefficients determined purely from the measurements of the pressure due to permanent gas products at two different lengths of the positive column are exhibited in Table 5. The values of dissociation coefficients listed here conform well to those obtained by the methods presented above. The most readily comparable value appearing in both Tables 4 and 5 is the rate coefficient evaluated at an E/p of $39.8 \text{ v}\cdot\text{cm}^{-1}\cdot\text{Torr}^{-1}$ for a gas pressure of 1.03 Torr. The slope of the $\Delta(\text{H}_2\text{O})/\Delta t$ vs. l plot yields a coefficient of 0.31, and the slope obtained by considering the time rates of appearance of noncondensable gas products in a given segment of the positive column leads to a coefficient of 0.35. The latter value is about 12 per cent greater than the former. This deviation is certainly within experimental error, especially when the steep rise in the rate coefficients with respect to rather small changes in the E/p values is considered.

All the results presented in the preceding were obtained at a discharge current of 0.5 mA. By the same method of measurements as the one employed in producing the coefficients given in Table 5, dissociation coefficients obtained with a variation in the discharge current are shown in Table 6.

Table 4. Dissociation coefficients for water vapor from the slopes of the $\Delta(H_2O)/\Delta t$ vs. λ plots.

P (torr)	1.03	1.72	3.64
$\Delta \lambda$ (cm)	15	22	5
Slope of $\Delta(H_2O)/\Delta t$ vs. λ plot ($\times 10^{-5}$ Torr \cdot sec $^{-1}$ \cdot cm $^{-1}$)	3.8	1.9	1.0
B/ip ($\times 10^5$ cm 3 \cdot amp $^{-1}$ \cdot Torr $^{-1}$)	15.7	9.4	4.5
E/p (v \cdot cm $^{-1}$ \cdot Torr $^{-1}$)	39.8	36.6	33.2
α_d/p (electron $^{-1}$ \cdot cm $^{-1}$ \cdot Torr $^{-1}$)	0.31	0.10	0.02

Table 5. Dissociation coefficients of water vapor on the basis of the reaction mechanism suggested by Figs. 12 and 13 and the corresponding expression for $(\alpha/p) = f(E/p)$ given in Eq. (IV.2).

P (Torr)	0.56	0.68	1.03	1.51	2.17
Δz (cm)	15	20	15	10	10
$\frac{2}{3} \left(\frac{\Delta P_2}{\Delta t} - \frac{\Delta P_1}{\Delta t} \right)$ (mTorr/sec)	0.68	0.77	0.65	0.31	0.23
B/ip ($\times 10^5 \text{ cm}^3 \cdot \text{amp}^{-1} \cdot \text{Torr}^{-1}$)	28.9	23.8	15.7	10.7	7.5
E/p ($\text{v} \cdot \text{cm}^{-1} \cdot \text{Torr}^{-1}$)	42.8	40.0	39.8	38.4	35.7
α_d/p ($\text{electron}^{-1} \cdot \text{cm}^{-1} \cdot \text{Torr}^{-1}$)	0.68	0.47	0.35	0.17	0.09

Table 6. Dissociation coefficients of water vapor with a variation in the discharge current, measured by the same method as those listed in Table 5.

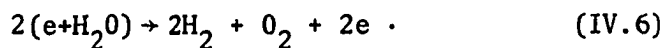
P (Torr)	0.59	0.93	1.23	1.39	1.89
i (mA)	0.25	0.25	0.25	0.7	0.7
Δl (cm)	15	15	15	15	10
$\frac{2}{3} \left(\frac{\Delta P_2}{\Delta t} - \frac{\Delta P_1}{\Delta t} \right)$ (mTorr/sec)	0.31	0.27	0.21	0.99	0.31
B/ip ($\times 10^5 \text{ cm}^3 \cdot \text{amp}^{-1} \cdot \text{Torr}^{-1}$)	54.7	34.7	26.3	8.3	6.1
E/p ($\text{v} \cdot \text{cm}^{-1} \cdot \text{Torr}^{-1}$)	41.3	39.4	39.0	38.4	36.0
α_d/p ($\text{electron}^{-1} \cdot \text{cm}^{-1} \cdot \text{Torr}^{-1}$)	0.58	0.33	0.195	0.29	0.10

The values of α_d/p measured with a change in the current are consistent with the measurements made at 0.5 mA, although it must be emphasized that the order of magnitude of the discharge current could not be lowered. It can be said, however, that the process leading to dissociation of water vapor must proceed by single encounters between electrons and molecules since the rate coefficients describing such a process are independent of current at least in the lower range characteristic of a normal glow discharge.

The dissociation coefficients measured, which all represent a first-order reaction, are plotted as a function of E/p in Fig. 14.

Dissociation Processes in H_2O

The 3:1 ratios obtained for the slopes given in Table 3 lead to the conclusion that three permanent gas molecules are formed in the positive column from every two dissociated H_2O molecules, providing that no condensable products arise as a result of dissociating collisions. Assuming the validity of such a proviso, the final reaction products may only consist of H_2 and O_2 molecules. Therefore, the overall reaction must be



The reaction given in Eq. (IV.6) was also concluded by Linder⁽²⁹⁾, who measured the dissociation rates in water vapor. His experiment employed flowing gas in what was believed to be a fully-

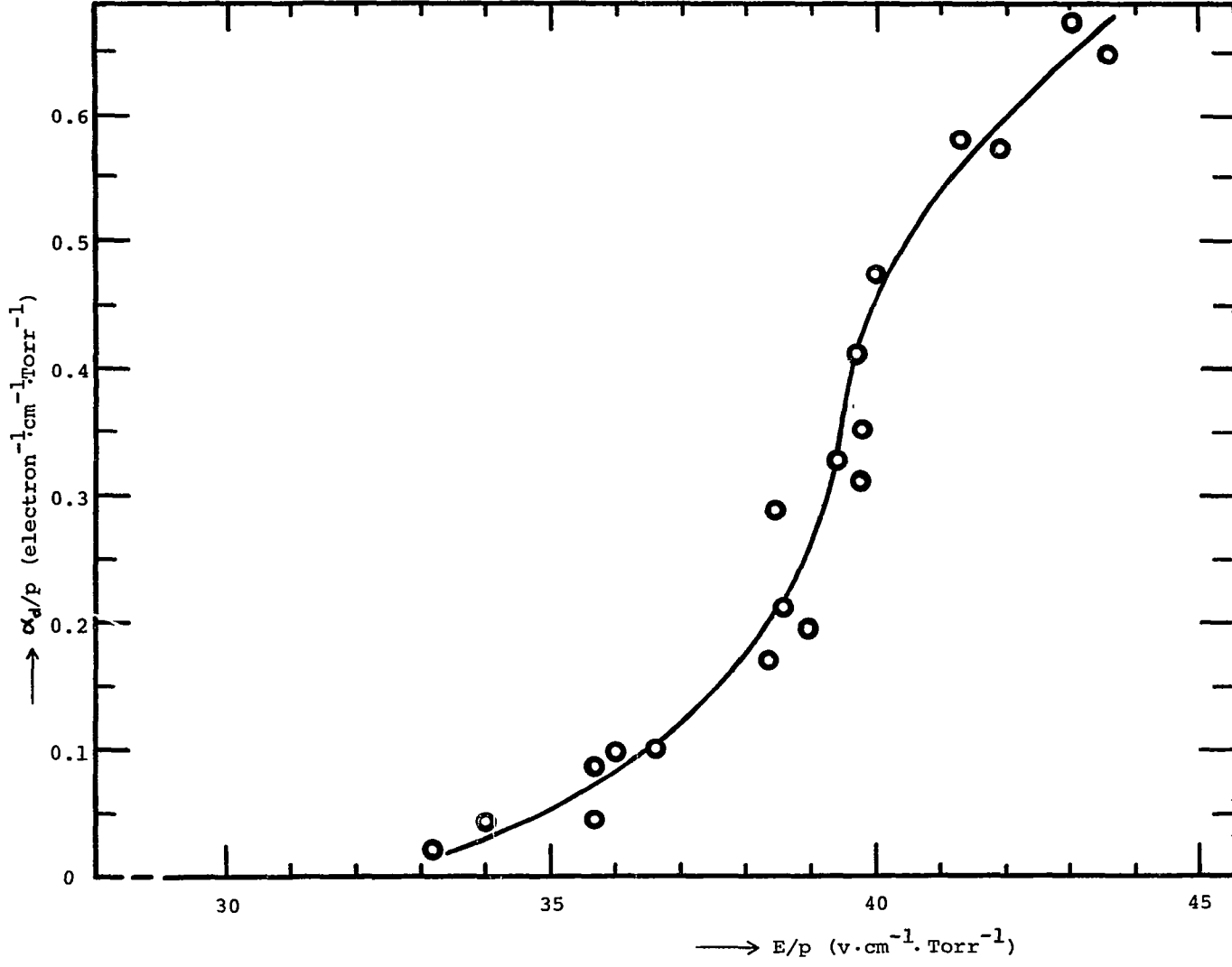


FIGURE 14. The Dissociation Coefficient of H₂O Vapor as a Function of E/p.

structured glow discharge and used a discharge tube, 6 cm in diameter, which had plane electrodes, each of a diameter of 3 cm. The values of discharge current ranged between 1 and 28 mA, and the interelectrode separation was varied from 1 to 9.75 cm. The pressure of the flowing gas was 0.75 Torr. A chemical analysis of the collected dissociation products revealed two molar parts of hydrogen, one of oxygen, and only a very small trace of hydrogen peroxide.

Unfortunately, it is not possible to make a meaningful comparison between the rates measured by Linder and those presented here. Linder described a glow discharge in which the positive column was "not visible". This observation, in view of the experimental conditions described above, clearly implies an almost complete absence of the column for discharge path lengths less than 10 cm. In a tube with plane electrodes, the Faraday dark space certainly tends to approach the anode, and the positive column is confined to the immediate vicinity of the anode. Consequently, the dissociation rates obtained by Linder appear to be almost entirely due to dissociation that takes place in all discharge regions, except the positive column.

The ionization coefficients for water vapor α_i/p , according to the measurements of Prasad and Craggs⁽³⁰⁾, have the same order of magnitude in the corresponding range of E/p as the dissociation coefficients displayed in Fig. 14. Therefore, it cannot be said, as it has been in the case of CO_2 , that the dissociation of water vapor proceeds predominantly by the route of dissociative excitation such that the

resulting fragments are electrically neutral. Moreover, water vapor is a strongly electronegative gas, and it is known to have attachment coefficients of the same order of magnitude as the ionization coefficients in the (E/p) -range of interest.

The attachment coefficient for electrons in water vapor α_a/p has been measured by Crompton, Rees, and Jory⁽³¹⁾ for the range of E/p between 20 and 60 $v \cdot \text{cm}^{-1} \cdot \text{Torr}^{-1}$. Furthermore, the cross section for dissociative attachment for H_2O has been obtained by Compton and Christophorou⁽³²⁾. This cross section for the formation of atomic-hydrogen negative ions has an onset energy of 5.7 eV, reaches a maximum of $6.9 \times 10^{-18} \text{cm}^2$ at 6.5 eV, then it rapidly decreases through a small secondary maximum of $1.3 \times 10^{-18} \text{cm}^2$ at 8.3 eV.

The attachment coefficient from this electron-capture cross section was calculated using a Maxwellian energy distribution. The values of drift velocity were taken from the data of Bailey and Duncanson⁽³³⁾, and the electron temperatures from the measurements of Crompton *et al.*⁽³¹⁾. The resulting attachment-coefficient curve is shown in Fig. 15 (marked as $\alpha(\text{H}^-)/p$) along with the attachment coefficient of Crompton, Rees, and Jory [$\alpha_a/p(\text{CR\&J})$]. The two curves agree in shape very well, but $\alpha(\text{H}^-)/p$ lies somewhat higher than α_a/p ; this discrepancy may be due either to uncertainties in the auxiliary data used, or to those in the magnitude of the measured cross sections.

The most likely mechanism⁽³⁴⁾ for the attachment process expressed by these attachment coefficients is believed to be

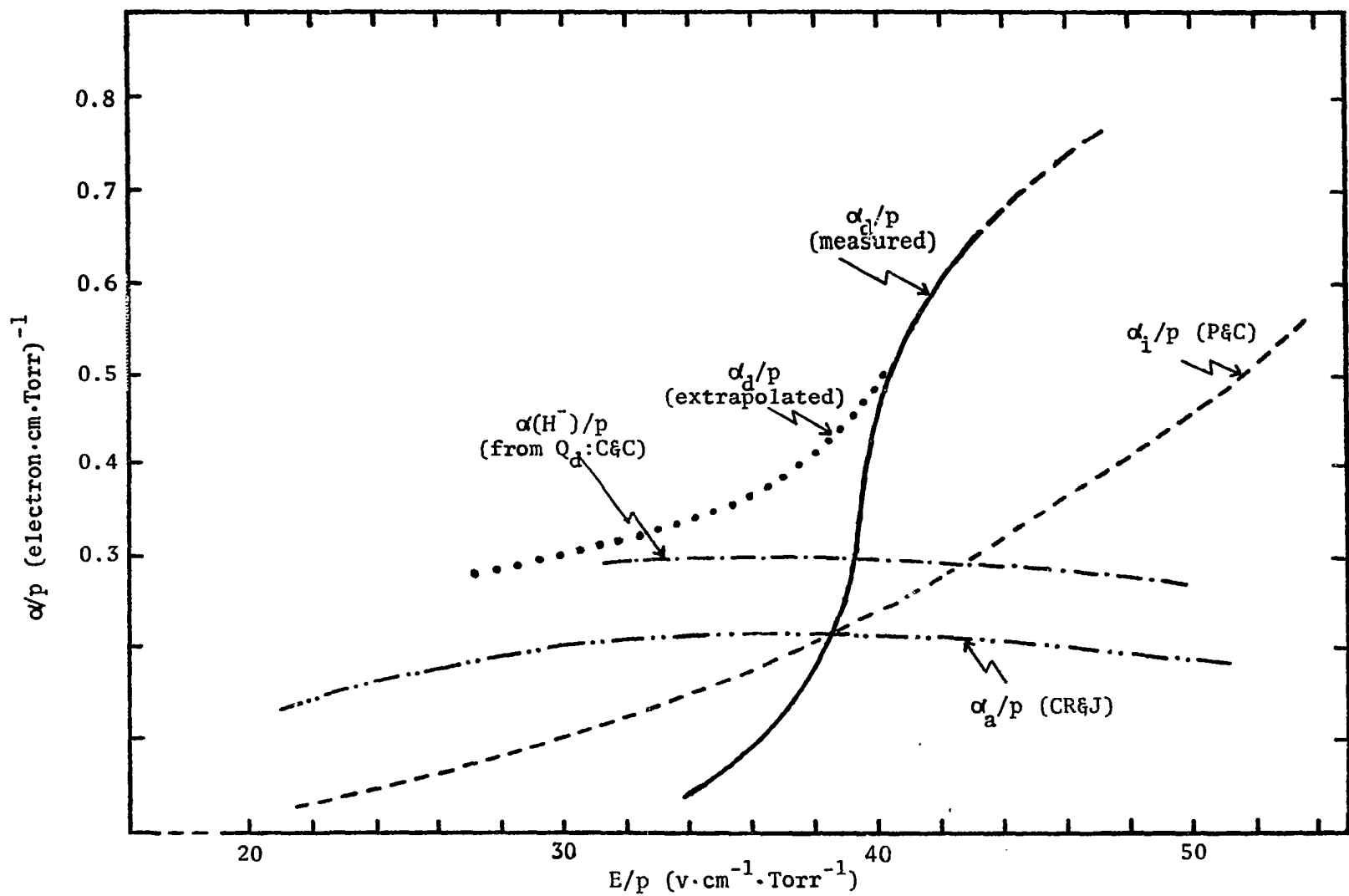
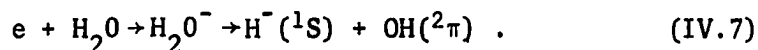


FIGURE 15. A Comparison of Dissociation Coefficients with Coefficients of Dissociative Attachment and Ionization.



This reaction mechanism significantly contributes to the net dissociation occurring in the positive column. The mean curve for the rate coefficients presented in Fig. 14 is reproduced in Fig. 15 along with the attachment and ionization coefficients for purposes of comparison.

The most striking feature of the (α_d/p) -curve is its very sudden rise from an E/p of about $32 \text{ v}\cdot\text{cm}^{-1}\cdot\text{Torr}^{-1}$. Since the ionization potential of the H_2O molecule is 12.6 eV, a comparison of α_d/p with α_i/p hints that the onset energy for such a steeply rising dissociation coefficient is well in excess of 12.6 eV. It is much more likely that H_2O vapor is dissociated by processes involving much less than such a high energy. Another surprising feature of the dissociation-coefficient curve is that it dips below the attachment coefficients at an E/p of about 39.5.

An appraisal of the possible mechanisms, in addition to the process of attachment given in (IV.7), that define the measured rate coefficients would be highly speculative. It is, however, not altogether unlikely that below an E/p of about 40 due to the excess negative ions, presumably H^- , which may in turn produce negative hydroxyl radicals through charge exchange, a recombination process takes place. Thus, water molecules may be re-formed. If such is the case, then recombination masks a "true" dissociation coefficient which possibly is roughly approximated by the dotted line in Fig. 15.

CHAPTER V

DISSOCIATION CROSS SECTION CALCULATED FROM SWARM DATA

It has been stated at the outset that the rate of a collision process depends upon an overlap integral between the energy distribution of electrons and the cross section for that process. Therefore, at least in principle, the measurement of the rate coefficient of dissociation makes it possible to obtain the corresponding cross section, provided that the electron-energy distribution is known. In order to accomplish this purpose, the overlap integral describing a rate process will be derived in a suitable form. The conventional arguments justifying the choice of the Maxwellian distribution will be cited and this distribution function is assumed in order to provide an assistance in giving a reasonable estimate of the magnitude and shape of the cross section for the dissociative excitation of CO_2 .

It has been also argued that the measured rate coefficient is dependent on the parameter E/p only if the electron-drift velocity and the mean electron energy are functions of E/p . The cross section and the distribution function are energy dependent only and are independent of pressure and electron concentration. In line with the theory of Emel us, Lunt and Meek, the invariance of the cross section

and electron-velocity distribution with pressure and electron concentration accounts for a principal characteristic of a chemical effect initiated by electron impact: the rate coefficient in glow discharges is often constant over considerable ranges of pressure and current density⁽⁴⁾. The experiments described in the preceding have again borne out that conditions in which a rate coefficient can be defined are satisfactorily met in a uniform positive column.

The Relation Between the Rate Coefficient and
the Cross Section

When an electron of known velocity v enters a space containing a concentration N molecules per unit volume and is driven by a uniform electric field, it may penetrate the gas by a distance x without encountering a molecule. The probability that it will collide with a molecule in traversing a path between x and $x + dx$ is expressed by the quantity $NQdx$, Q being the hypothetical target area, the cross section, that is exposed by a molecule to an impinging electron to effect a particular collision process. Hence, the number of species produced per unit time as a result of impacts between molecules and an electron having a velocity v is vNQ .

However, since an electron swarm is considered here, the electrons move with a distribution of velocities $f(v)dv$ per unit volume in equilibrium with the applied electric field: the ones losing a fraction of their energy upon collisions will fall back

to lower regions of the energy distribution while others of lower velocities are being accelerated. Therefore, the differential rate of production of species per unit volume in the swarm is

$$dn = NQvf(v)dv . \quad (V.1)$$

The number of events per unit time is proportional to the number density of electrons N_e drifting in the direction of the field and the velocity of the drift motion w the magnitude of which determines the rate of electron-energy gain from the field. Hence,

$$dn = d\alpha N_e w . \quad (V.2)$$

By combining Eqs. (1) and (2), $d\alpha$, which expresses the number of events produced by electrons drifting unit length along the field and having velocities lying between v and $v + dv$, is found as

$$d\alpha = \frac{Nv}{N_e w} Q(v)f(v)dv . \quad (V.3)$$

The question of what type of distribution function $f(v)$ is to be employed in Eq. (V.3) cannot be answered in general. The distribution depends on the nature of gas in which a particular process takes place and the range of electric field applied. However, it can be said in view of strong evidence, in not too complex molecular gases (e.g., carbon dioxide) and for intermediate values of the applied electric field the electron-energy distribution is closely Maxwellian⁽³⁵⁾.

It is to be emphasized that the Maxwellian distribution law is strictly applicable only in cases in which the interaction between the electrons through mutual repulsion is the main cause of the rearrangement of electronic energies, i.e., when the current densities are high. However, a number of investigations have shown^(2,36) that in molecular gases the Maxwellian distribution is often a good approximation, even when the current densities are small. Large departures occur at high values of E/p and at very small currents.

Ionization and excitation are processes that depend upon the number of electrons in the high-energy tail of the distribution, while transport phenomena, diffusion and drift, depend on the mean electron energy. The reason why the electronic velocity distribution in molecular gases can be approximated closely as Maxwellian lies in the fact that the excitation levels in these gases are widely spread out to the ionization potential and thus, inelastic losses occur at quite low energies. The mean electron energy is low, but the losses are distributed such that the resulting distribution is closely Maxwellian. In atomic gases the excitation levels are much closer to the ionization potential, and at low values of E/p only the elastic losses are prominent. The mean energy is much higher than in molecular gases at the same E/p , hence, the number of high-energy electrons is depleted. In addition, the Ramsauer-Townsend effect further enhances the deficiency of high-energy electrons. In molecular gases, in general, the mean free paths change relatively slowly with electron energy.

For these reasons the Maxwellian velocity distribution⁽³⁷⁾ is chosen to specify the distribution function in Eq. (V.3):

$$f(v)dv = \frac{4N_e}{\sqrt{\pi}} \left(\frac{v}{v_m}\right)^2 \exp\left[-\left(\frac{v}{v_m}\right)^2\right] d\left(\frac{v}{v_m}\right) . \quad (V.4)$$

This distribution now defines the probability that a randomly selected swarm electron will have a value of velocity between v and $v + dv$. The maximum of the distribution curve occurs at v_m , the most probable velocity of swarm electrons. Noting that $d(v/v_m) = dv/v_m$, an insertion of Eq. (V.4) into Eq. (V.3) yields for the rate coefficient α the expression integrated over all velocities:

$$\alpha = \frac{4N}{\sqrt{\pi w}} \int_0^{\infty} Q(v) \left(\frac{v}{v_m}\right)^3 \exp\left[-\left(\frac{v}{v_m}\right)^2\right] dv . \quad (V.5)$$

Since the gas density N is Lp , where L is the Loschmidt number, the rate coefficient per unit pressure becomes

$$\frac{\alpha}{p} = \frac{c}{w} \int_0^{\infty} Q(v) \left(\frac{v}{v_m}\right)^3 \exp\left[-\left(\frac{v}{v_m}\right)^2\right] dv . \quad (V.6)$$

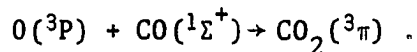
The constant c resulting from the numerical factors has a value very close to 8×10^{16} . Equation (V.6) then enables one to determine the energy-dependent cross section if the rate coefficient is measured as a function of E/p , and if data are available for the (E/p) -dependent quantities, the drift velocity and electron temperature.

The Dissociation Cross Section of CO₂

As a comparison of Figs. 8 and 9 has shown, carbon dioxide must dissociate into neutral species. Considering that the dissociation energy of CO₂ is 5.5 eV while its ionization energy is 14.4 eV, this result is to be expected. In order to arrive at the observed values of α_d/p at low values of E/p, dissociation must be produced by electrons of much lower energy than that needed for ionization. Very many more such slow electrons are present in the positive column than electrons of high energy which contribute to the ionization.

It is probable that the state in which the CO₂ molecule spontaneously dissociates has a vertical excitation energy that is very little greater than the actual thermal dissociation energy of CO₂.

It was suggested by Laidler⁽³⁸⁾ that a $^3\pi$ state of CO₂ lies at about 6.07 eV above the minimum of the ground state when the schematic potential-energy surfaces for the system O-C-O were considered to explain the kinetics of the impact-reaction,



I.e., when an oxygen atom in its lowest (3P) state approaches a carbon monoxide molecule in its lowest ($X^1\Sigma^+$) state, the resulting state is an excited carbon dioxide molecule. In the corresponding potential profile the most populated levels of the lowest state are separated by about 6.07 eV from the upper surface.

Excitation to this state, which dissociates into CO and O, would seem to be consistent with the observed reaction in the CO₂ positive-column experiment. While dissociation leading to a low-lying excited state of the oxygen atom may be occurring, it seems inconceivable that an excited CO could be involved since this would require an excess energy of at least 6 eV above the dissociation energy of CO₂, making a total of 11.5 eV. The rate coefficient for such a reaction would almost certainly be of the order of magnitude of the ionization coefficient.

In order to make an estimate of the magnitude and shape of an excitation cross section, which is indeed consistent with the experimentally determined dissociation coefficient, the method of estimation given by Eq. (V.6) was applied.

The following values of electron drift velocities w and the ratio of electron to gas temperatures (the Townsend energy factor k)⁽³⁹⁾ were used to construct the Maxwellian distribution of velocities.

w ($\times 10^6$ cm/sec)	11.2	14.8	16.6
T_e/T_g	42.3	76.8	95
E/p ($v \cdot \text{cm}^{-1} \cdot \text{Torr}^{-1}$)	10	20	30

The values taken for both the drift velocities and electron-to-gas temperature ratios above an E/p of $15 v \cdot \text{cm}^{-1} \cdot \text{Torr}^{-1}$ were obtained by extrapolation. In obtaining the extrapolated values, Riemann's value for the drift velocity at an E/p of $36 v \cdot \text{cm}^{-1} \cdot \text{Torr}^{-1}$ measured by the cloud-chamber method was also taken into account⁽⁴⁰⁾.

Since the mean random velocity of electrons is defined by $mv_r^2/2 = 3kT_e/2$, and the most probable velocity is $v_m = 0.816 v_r$ for the Maxwellian function, Eq. (V.6) made it possible to obtain calculated values of the dissociation coefficient. The overlap between the initially assumed and subsequently corrected cross sections and the appropriate distribution function was numerically integrated, so that the values of the dissociation coefficients calculated in this manner were made, within experimental error, coincident with the measured values. These coefficients are compared in the following:

E/p_0 ($v \cdot \text{cm}^{-1} \cdot \text{Torr}^{-1}$)	10	20	30
$(\alpha_d/p_0)_{\text{calc.}}$	0.077	0.46	0.63
$(\alpha_d/p_0)_{\text{obs.}}$	0.07	0.43	0.67

The cross section yielding the calculated values of α_d/p_0 clearly indicates that the observed dissociation coefficients can be explained by a singlet-to-triplet type of excitation function. As shown in Fig. 16, it rises from an onset potential of 6.1 eV to a peak of about $3.5 \times 10^{-17} \text{cm}^2$ at an energy of 6.9 eV and then decreases very rapidly through a value of $1.2 \times 10^{-17} \text{cm}^2$ at 7.7 eV.

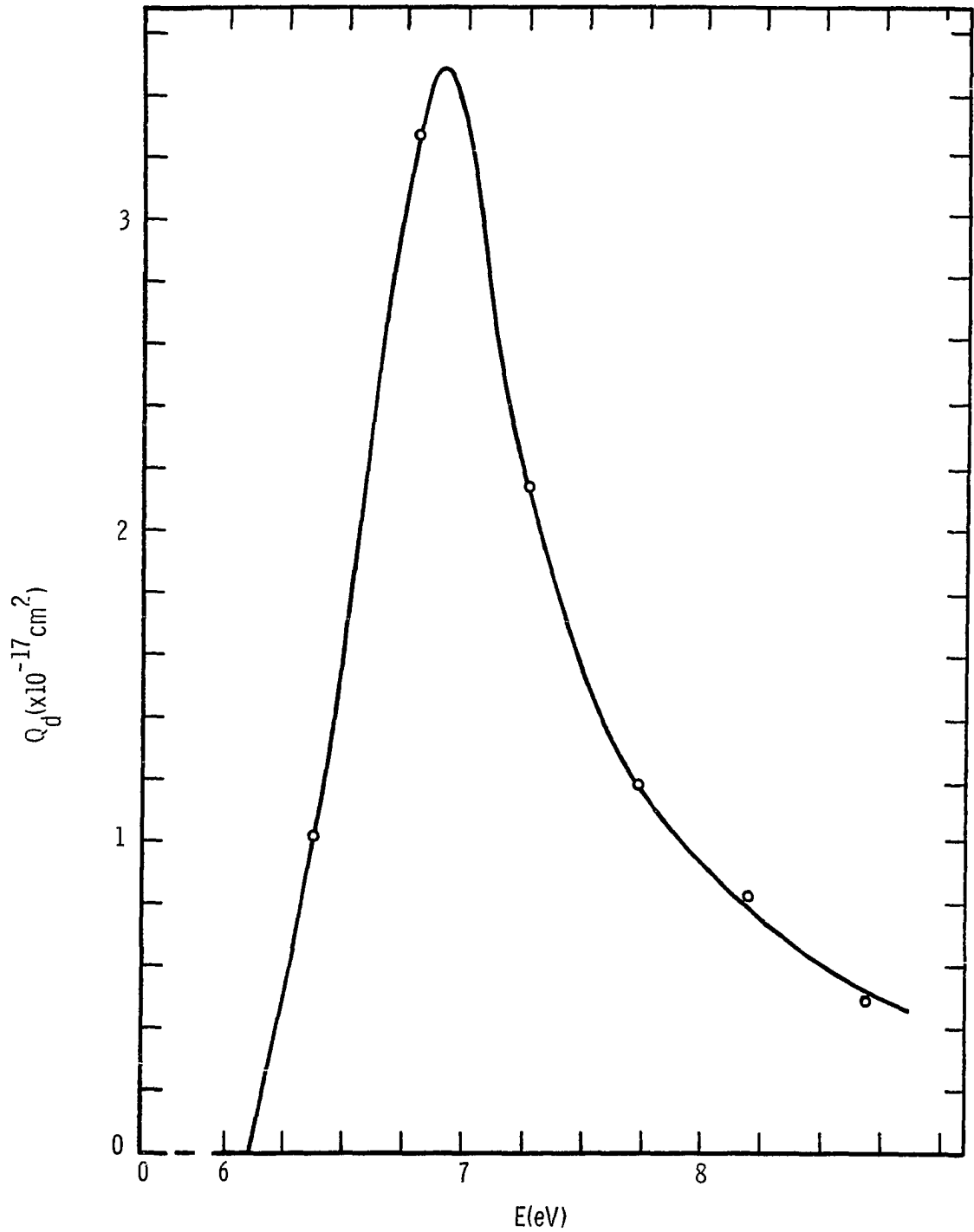


FIGURE 16. The Estimated Electron-Impact Dissociation Cross Section for CO_2 as a Function of Electron Energy E .

CHAPTER VI

SUMMARY

The quantitative investigation of dissociation in carbon dioxide and water vapor used the uniform positive column of a dc glow discharge in a static system and employed the method of separation of permanent dissociation products from the condensable parent gas. The experimental conditions were designed to be such that a steady-state swarm was assured in the positive column, and the events observed there could be distinguished from the effects of all other glow-discharge regions. Conditions were established in which the accumulation of dissociation products were minimized and thus, it was possible to obtain the reduced field E/p of the positive column as a function of the reduced tube radius pR in essentially pure carbon dioxide and water vapor. The dissociation of CO_2 was investigated for gas pressures between 0.3 and 4 Torr; the range of pressures available in the H_2O positive column for similar measurements was between 0.4 and 4 Torr. The current employed was varied between 0.3 and 0.7 mA, and it was shown that the dissociation of both CO_2 and H_2O vapor resulted from single collision between electrons and molecules.

The number of dissociating collisions α_d/p by an electron drifting unit length along the field direction of the positive column was measured for both gases. In CO_2 these rate coefficients were found for values of E/p between 11 and 32 $\text{v}\cdot\text{cm}^{-1}\cdot\text{Torr}^{-1}$, the values of α_d/p were 0.15 and 0.67 at these limits. The rate coefficients of dissociation for water vapor ranged between 0.025 at an E/p of 34 and 0.65 at an E/p of 43 $\text{v}\cdot\text{cm}^{-1}\cdot\text{Torr}^{-1}$.

These experiments demonstrated that the dissociation of CO_2 was an electron-impact reaction resulting in an excited state for the molecule followed by a fragmentation into uncharged species, CO and O . The measurements suggested a mechanism for the reaction. Assuming the validity of the Maxwellian energy-distribution for this gas, a dissociation cross section was calculated. It was suggested that the dissociative excitation was to a $^3\pi$ state of CO_2 about 6.1 eV above the ground state. With an onset of 6.1 eV, a cross section rising to a maximum of $3.5 \times 10^{-17} \text{cm}^2$ at 6.9 eV and then rapidly decreasing with increasing electron energies, proved to be consistent with the experimentally determined dissociation-rate coefficients.

The results obtained for the dissociation of water vapor showed that the resulting products consisted of H_2 and O_2 . The magnitude of the dissociation coefficients measured was of the same order as the magnitude of attachment coefficients, hence, negative ion formation must play an important role in the positive column. The measurements also indicated that processes involving ionized species might strongly influence the net chemical change occurring in the discharge. At E/p less

than $40 \text{ v}\cdot\text{cm}^{-1}\cdot\text{Torr}^{-1}$ negative hydroxyl ions might be instrumental in a fast recombination of water molecules, and above this value of E/p , an increasingly rapid production of oxygen and hydrogen molecules was seen, presumably as a result of dissociation of water into free atoms and a subsequent recombination to form H_2 and O_2 . Since the observed rate coefficients described an overall dissociation process, the relative contributions of the simultaneous processes leading to dissociation could not be ascertained in the present experiments.

LIST OF REFERENCES

1. J. S. Townsend, Electricity in Gases (Clarendon Press, Oxford, 1915) p. 266 ff.
2. K. G. Emeléus, R. W. Lunt and C. A. Meek, Proc. Roy. Soc. (London) A156, 394 (1936).
3. R. W. Lunt and C. A. Meek, ibid. A157, 146 (1936).
4. R. W. Lunt, Rep. Progr. Phys. 8, 338 (1941).
5. H. G. Poole, Proc. Roy. Soc. (London) A163, 424 (1937).
6. S.J.B. Corrigan and A. von Engel, Proc. Roy. Soc. (London) A245, 335 (1958).
7. T. M. Shaw, J. Chem. Phys. 30, 1366 (1959).
8. S.J.B. Corrigan, J. Chem. Phys. 43, 4381 (1965).
9. S.J.B. Corrigan, Private communication.
10. See, for example, G. Glockler and S. C. Lind, The Electrochemistry of Gases and other Dielectrics (John Wiley & Sons, Inc., New York, 1939).
11. N. N. Sobolev and V. V. Sokovikov, in The Physics of Electronic and Atomic Collisions: Invited Papers from the 5th International Conference, Leningrad, July 17-23, 1967. (L. M. Branscomb, ed.) pp. 49-60.
12. J. S. Townsend, Motion of Electrons in Gases (Clarendon Press, Oxford, 1925).

13. L. B. Loeb, Basic Processes of Gaseous Electronics (The California University Press, Berkeley, 1955), Chapters 1, 2 and 3.
14. S. Chapman and T. G. Cowling, The Mathematical Theory of Non-Uniform Gases (Cambridge University Press, 1939).
15. C. Kenty, Rev. Sci. Instr. 17, 158 (1946).
16. M. Pirani and J. Yarwood, Principles of Vacuum Engineering (Reinhold Publishing Corp., New York, 1961).
17. R. Holmes and G. R. Jones, Vacuum 13, 231 (1963).
18. W. E. Deming, Statistical Adjustment of Data (John Wiley & Sons, Inc., New York, 1943) p. 167 ff.
19. A. von Engel, Ionized Gases, Second Ed. (Clarendon Press, Oxford, 1965), p. 217 ff.
20. G. Francis, The Glow Discharge at Low Pressure (in Handbuch der Physik, vol. XXII, pp. 53-208, Springer-Verlag, Berlin, 1956).
21. R. Seeliger and A. Wichmann, Ann. Phys. 9, 235 (1951).
22. R. Seeliger, Z. Naturforsch. 8a, 74 (1953).
23. G. Francis, op.cit., p. 119.
24. A. Güntherschulze, Z. Phys. 42, 763 (1927).
25. G. J. Schulz, Phys. Rev. 128, 178 (1962).
26. D. Rapp and D. D. Briglia, J. Chem. Phys. 43, 1480 (1965).
27. Data of D. R. Young, cited by S. C. Brown, Basic Data of Plasma Physics (MIT Press, Cambridge, Mass., 1959), p. 129.
28. Cf. J. H. de Boer, The Dynamical Character of Adsorption, Second Ed. (Clarendon Press, Oxford, 1968).

29. E. G. Linder, *Phys. Rev.* 38, 679 (1931).
30. A. N. Prasad and J. D. Craggs, *Proc. Phys. Soc.* 76, 223 (1960).
31. R. W. Crompton, J. A. Rees and R. L. Jory, *Austral. J. Phys.* 18, 541 (1965).
32. R. N. Compton and L. G. Christophorou, *Phys. Rev.* 154, 110 (1967).
33. V. A. Bailey and W. E. Duncanson, *Phil. Mag.* 10, 145 (1930), cited by R. H. Healey and J. W. Reed, *The Behavior of Slow Electrons in Gases* (Amalgamated Wireless, Sydney, 1941), p. 99.
34. K. J. Laidler, *J. Chem. Phys.* 22, 1740 (1954).
35. For a discussion of the applicability of Maxwellian distribution, see A. von Engel, *Ionization in Gases by Electrons in Electric Fields* (in *Handbuch der Physik*, vol. XXI, Springer-Verlag, Berlin, 1956) p. 539 ff.; L. B. Loeb, *op.cit.*, p. 712 ff.
36. H. D. Deas and K. G. Emeléus, *Phil. Mag.* 11, 460 (1949).
37. A. von Engel, *Ionized Gases*, *op.cit.*, p. 292.
38. K. J. Laidler, *The Chemical Kinetics of Excited States* (Clarendon Press, Oxford, 1955), p. 79.
39. Data of J. B. Rudd and M. F. Skinker cited by R. H. Healey and J. W. Reed, *The Behavior of Slow Electrons in Gases* (Amalgamated Wireless, Sydney, 1941), pp. 98-99.
40. See L. B. Loeb, *op.cit.*, p. 258.